

RESEARCH ARTICLE

Cell-autonomous role of GFR α 1 in the development of olfactory bulb GABAergic interneurons

Sabrina Zechel^{1,*}, Diana Fernandez-Suarez¹ and Carlos F. Ibáñez^{1,2,3,4,‡}**ABSTRACT**

GFR α 1, a receptor for glial cell line-derived neurotrophic factor (GDNF), is critical for the development of the main olfactory system. The olfactory bulb (OB) of Gfra1 knockout mice shows significant reductions in the number of olfactory sensory neurons, mitral and tufted cells, as well as all major classes of OB GABAergic interneurons. However, the latter do not express significant levels of GFR α 1, leaving the mechanism of action of GFR α 1 in OB interneuron development unexplained. Here we report that GFR α 1 is highly expressed in the precursor cells that give rise to all major classes of OB interneurons, but is downregulated as these neurons mature. Conditional ablation of GFR α 1 in embryonic GABAergic cells recapitulated the cell losses observed in global Gfra1 knockouts at birth. GFR α 1 was also required for the sustained generation and allocation of OB interneurons in adulthood. Conditional loss of GFR α 1 altered the migratory behaviour of neuroblasts along the rostral migratory stream (RMS) as well as RMS glial tunnel formation. Together, these data indicate that GFR α 1 functions cell-autonomously in subpopulations of OB interneuron precursors to regulate their generation and allocation in the mammalian OB.

KEY WORDS: Cell migration, RMS, SVZ**INTRODUCTION**

In the mammalian forebrain, most subpopulations of GABAergic interneurons originate in distant neurogenic areas and migrate to their final locations following trajectories that are, for the most part, tangential to the brain surface. In the developing olfactory system, OB interneuron precursors are generated in the lateral ganglionic eminences, subventricular zone (SVZ) and septum of the embryonic forebrain, and migrate rostrally to the OB through a cell migration pathway known as the rostral migratory stream (RMS) (Lois and Alvarez-Buylla, 1994; Luskin, 1993, 1998; Wichterle et al., 2001). In the glomerular layer (GL) of the OB, interneurons expressing tyrosine hydroxylase (TH), calbindin (CB) and calretinin (CR) are generated sequentially in waves during early embryonic stages, later

embryonic stages and postnatal stages, respectively (Batista-Brito et al., 2008). In the mouse embryo, the LGE and the septum were reported to give rise to different types of OB interneurons. While the septum generated mostly GL CR-positive cells, the LGE produced all major GL subpopulations, as well as CR interneurons destined to the granule cell layer (GR) (Qin et al., 2017). At birth, the majority of cells in the GR are CR-positive (Batista-Brito et al., 2008). OB GABAergic interneurons are one of the few neuronal subpopulations that is continuously renewed throughout life from progenitors located in the adult SVZ (Altman et al., 1969; Lledo et al., 2006). Within the adult SVZ, there is considerable heterogeneity and the location of progenitor cells has been shown to determine the types of OB interneurons they generate (Azim et al., 2012; Merkle et al., 2007). In the mouse, it has more recently been shown that the majority of progenitor cells in the adult SVZ (i.e. B cells) are produced during midembryogenesis, and remain quiescent until they become reactivated postnatally (Fuentelba et al., 2015). Despite significant progress, the molecular signals that control the generation, migration, allocation and differentiation of GABAergic interneurons destined for the OB are incompletely understood.

The neurotrophic factor GDNF was initially discovered as a survival factor for midbrain dopaminergic neurons (Lin et al., 1993). It signals by binding to the GPI-anchored receptor GFR α 1 (GDNF family receptor alpha 1) in complex with either the receptor tyrosine kinase RET (Treanor et al., 1996; Trupp et al., 1996) or the neural cell adhesion molecule (NCAM) (Paratcha et al., 2003). GFR α 1 is therefore an essential component of functional GDNF receptors. In the olfactory system, our laboratory has reported GFR α 1 expression in immature olfactory sensory neurons (OSNs) and olfactory ensheathing cells (OECs) of the olfactory epithelium (OE) (Marks et al., 2012). In the OB, GFR α 1 was found in projection neurons, namely mitral and external tufted cells, but was largely excluded from GABAergic interneurons (Marks et al., 2012). Knockout mice lacking GFR α 1 showed reduced numbers of OSNs, projection neurons, and all major OB interneuron subpopulations, including those marked by expression of TH, CB and CR (Marks et al., 2012). Thus, GFR α 1 would appear to play a role in OB interneuron development or maintenance even though it is not itself expressed at mature stages in those cells. Loss of GFR α 1 could affect OB interneuron development non-cell-autonomously, as an indirect consequence of defects in OSNs and projection neurons. Alternatively, GFR α 1 may initially be required for the development of OB interneuron precursors, but later downregulated in mature OB interneurons. GFR α 1 colocalizes with NCAM in RMS cells (Paratcha et al., 2003) and GDNF displays chemoattractant activities towards these cells in cell culture experiments (Paratcha et al., 2006). However, the *in vivo* physiological relevance of those observations has been unclear.

Here, using conditional deletion of GFR α 1, we show that this receptor functions transiently and cell-autonomously in subpopulations of OB interneuron precursors to regulate their

¹Department of Cell and Molecular Biology, Karolinska Institute, Stockholm 17177, Sweden. ²Department of Physiology, National University of Singapore, Singapore 117597, Singapore. ³Life Sciences Institute, National University of Singapore, Singapore 117456, Singapore. ⁴Stellenbosch Institute for Advanced Study, Wallenberg Research Centre at Stellenbosch University, Stellenbosch 7600, South Africa.

*Present address: Universitätsmedizin Göttingen, Department of Neuropathology, Robert-Koch-Str.40, 37075 Göttingen, Germany.

‡Author for correspondence (carlos.ibanez@ki.se)

 C.F.I., 0000-0003-1181-7641

This is an Open Access article distributed under the terms of the Creative Commons Attribution License (<http://creativecommons.org/licenses/by/3.0>), which permits unrestricted use, distribution and reproduction in any medium provided that the original work is properly attributed.

migration to the OB. We provide evidence showing that selective loss of $GFR\alpha 1$ in GABAergic precursors affects RMS glial tube formation and induces premature neuroblast differentiation, leading to losses in all major subpopulations of OB interneurons.

RESULTS

$GFR\alpha 1$ expression in OB GABAergic interneuron precursors of the embryonic septum, olfactory primordium and adult SVZ

The precursors of OB GABAergic interneurons are generated in the lateral ganglionic eminence (LGE), septum and olfactory primordium (OBp) during early embryonic stages and in the subventricular zone (SVZ) at later embryonic stages and throughout adulthood (Lois and Alvarez-Buylla, 1994; Luskin, 1993, 1998). In the embryonic septum and LGE, precursor cells expressing the Sp8 transcription factor can give rise to OB CR-expressing cells (Waclaw et al., 2006; Young et al., 2007). Previous studies had indicated that $GFR\alpha 1$ is not expressed in the LGE (Canty et al., 2009; Pozas and Ibáñez, 2005). We used $R1CG^{fx/fx}$ mice, which have been engineered to express green fluorescent protein (GFP) from the *Gfra1* locus upon Cre-mediated recombination (Uesaka et al., 2007). $R1CG^{fx/+};Ella^{Cre}$ mice express GFP in all $GFR\alpha 1$ -positive cells and retain one functional *Gfra1* allele. At embryonic day 12.5 (E12.5), GFP was detected in cells of the OBp and

developing septum, several of which also expressed Sp8 (Fig. 1A). These results confirm that $GFR\alpha 1$ is expressed in subpopulations of Sp8⁺ precursors localised to the septum and OBp. In order to identify cell precursors of OB interneurons in postnatal adult SVZ, we performed immunohistochemistry on sections through the lateral wall of the lateral ventricle and detected significant overlap between GFP and GABA (Fig. 1B). Together, these results indicated that $GFR\alpha 1$ is expressed in subpopulations of precursors of OB GABAergic interneurons at both embryonic and adult stages.

Precursors and neuroblasts expressing $GFR\alpha 1$ contribute to all major subpopulations of GABAergic interneurons in the newborn and adult OB

Next, we assessed the contribution of precursor cells expressing $GFR\alpha 1$ to the major classes of OB interneurons during both embryonic development and in the adult. We performed inducible genetic fate mapping by treating $Gfra1^{CreERT2/+};dTom$ pregnant females with Tmx at E10.5 and E11.5 and analysed the phenotypes of OB dTom-positive cells at birth (P0). We observed dTom-positive cells in the granule cell and glomerular layers of the newborn OB as well as a prominent dTom signal in the olfactory nerve layer (ONL) (Fig. 2A), in agreement with our previous studies (Marks et al., 2012). In the GL, dTom-positive cells were seen to co-express TH and CB, while in the GR, we detected co-expression

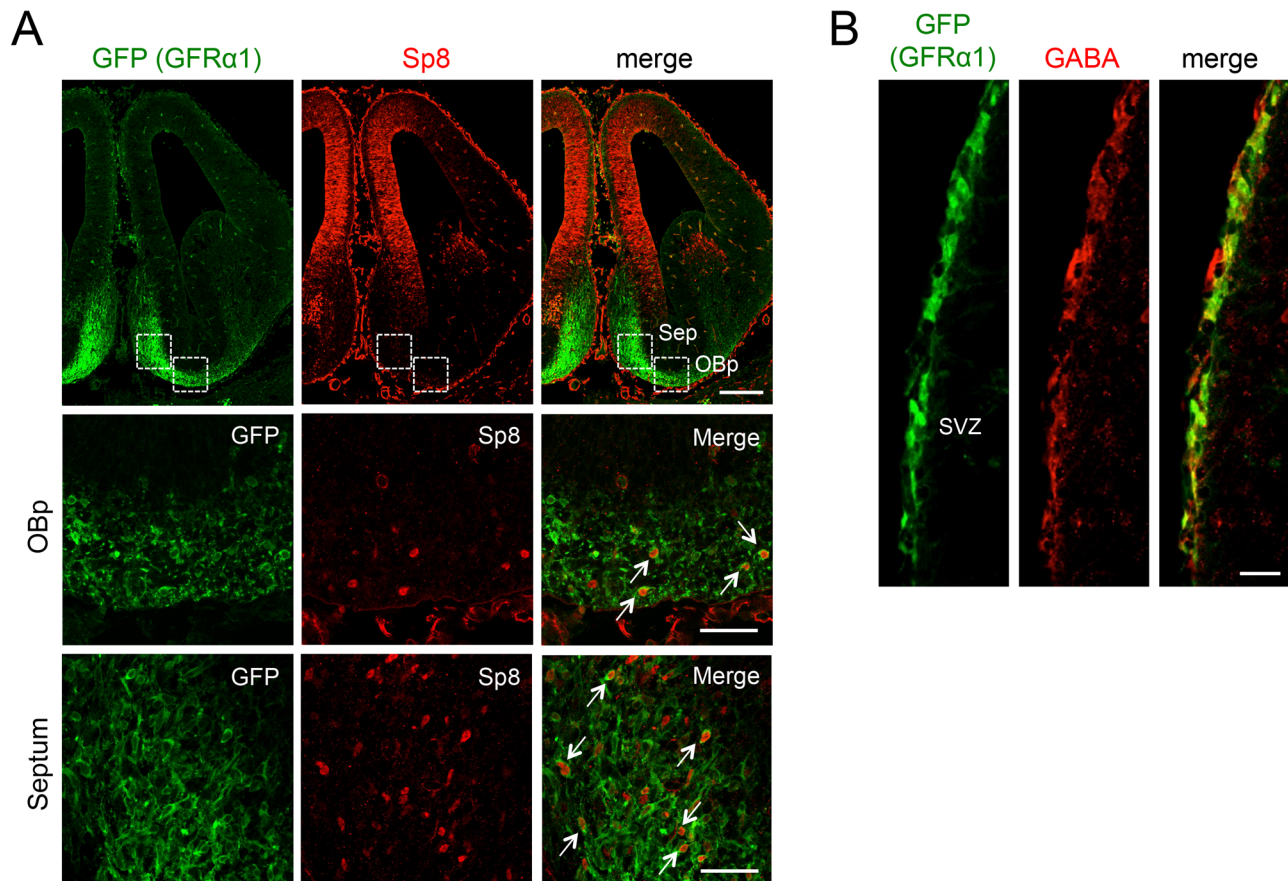


Fig. 1. $GFR\alpha 1$ expression in OB GABAergic interneuron precursors of the embryonic septum and adult subventricular zone (SVZ). (A) Expression of $GFR\alpha 1$ (green, visualised as GFP expression driven from the $R1CG$ locus after $Ella^{Cre}$ -mediated recombination) and Sp8 (red) detected by immunohistochemistry in cells of the olfactory primordium (OBp) and septum (sep) of E12.5 mouse embryos. The two lower rows display higher magnification images of the areas in septum and OBp indicated in the upper row. In four biological replicates, 65% of Sp8⁺ cells were also GFP⁺ in septum, and 35% in the OBp (arrows). OBp, olfactory primordium; Sep, septum. Scale bars: 200 μ m (upper row), 40 μ m (two lower rows). (B) Expression of $GFR\alpha 1$ (green, visualised as GFP) and GABA (red) detected by immunohistochemistry in the SVZ of the lateral ventricle in 7-week-old $R1CG^{fx/+};Ella^{Cre}$ mice. In five biological replicates, 80% of GABA⁺ cells were also GFP⁺. Scale bar: 30 μ m.

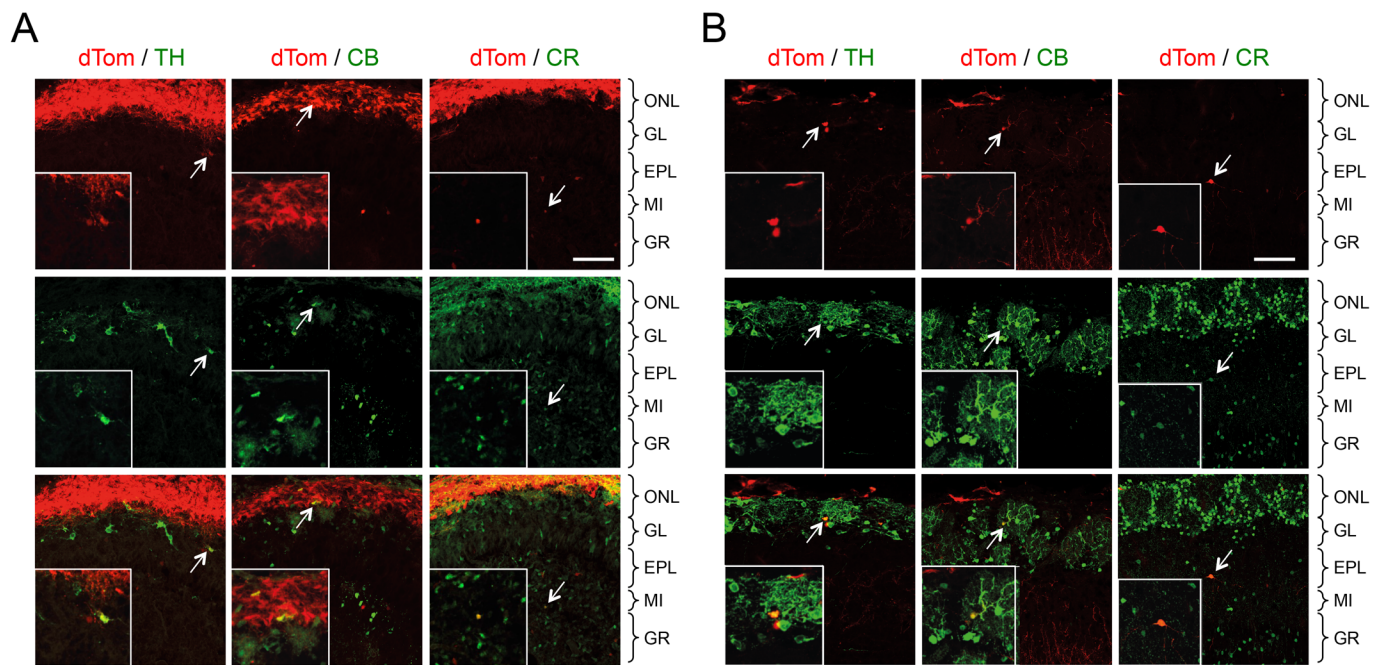


Fig. 2. Precursor cells expressing GFR α 1 contribute to all major subpopulations of GABAergic interneurons in the newborn and adult OB.

(A) Expression of dTomato (dTom) in the OB of newborn (P0) *Gfra1^{CreERT2/+};dTom* mice injected with Tamoxifen at E10.5 and E11.5. The lower panels show overlap of dTom labelled cells with OB GABAergic interneuron markers tyrosine hydroxylase (TH), Calbindin and Calretinin (arrows). Inserts show higher magnification of double-positive cells. The different OB layers are indicated on the right. In six biological replicates, 25% of TH⁺, 11% of CB⁺ and 15% of CR⁺ cells were also dTom⁺. ONL, olfactory nerve layer; GL, glomerular layer; EPL, external plexiform layer; MI, mitral cell layer; GR, granule cell layer. Scale bar: 50 μ m. (B) Expression of dTomato (dTom) in the OB of P56 *Gfra1^{CreERT2/+};dTom* mice injected with Tamoxifen at P21, P22 and P23. The lower panels show overlap of dTom labelled cells with OB GABAergic interneuron markers tyrosine hydroxylase (TH), Calbindin and Calretinin (arrows). Inserts show higher magnification of double-positive cells. The different OB layers are indicated on the right. In six biological replicates, 5% of TH⁺, 3% of CB⁺ and 30% of CR⁺ cells were also dTom⁺. ONL, olfactory nerve layer; GL, glomerular layer; EPL, external plexiform layer; MI, mitral cell layer; GR, granule cell layer. Scale bar: 50 μ m.

with CR (Fig. 2A). Because of the inherent limitations of Tmx-directed recombination, the contribution of precursor cells expressing GFR α 1 to these OB interneuron types could not be quantitatively determined from this analysis. Nevertheless, these results indicate that GFR α 1-expressing precursors in the embryo can give rise to all major classes of OB interneurons at birth. In order to study the progeny of adult GFR α 1-expressing precursor cells, we injected Tmx at P21, P22 and P23 and examined their OB fates at P56. Similar to embryonic precursors, we found that adult neuroblasts expressing GFR α 1 can give rise to interneurons expressing TH, CB or CR in the adult OB (Fig. 2B). Given that most OB interneurons do not themselves express GFR α 1 (Marks et al., 2012), we conclude that this receptor is transiently expressed in subpopulations of precursor cells and neuroblasts that later gives rise to OB interneurons through embryonic development and in the adult. GFR α 1 may contribute to different aspects of the development of OB interneuron precursors, such as proliferation, differentiation or migration, before being downregulated in mature OB interneurons.

Cell-autonomous loss of GABAergic interneurons in the OB of newborn and adult conditional GFR α 1 mutants

Our finding of GFR α 1 expression in embryonic and adult precursors of OB GABAergic neurons opened the possibility that a cell-autonomous, albeit transient, function of GFR α 1 in these precursors may regulate the final number of OB GABAergic interneurons. As the precursors of all TH- and CB-positive periglomerular cells, as well as the majority of CR-positive granule neurons, are also positive for GAD67 (Kosaka and

Kosaka, 2007; Sawada et al., 2011), we crossed mice expressing Cre recombinase from the *Gad67* locus (Tolu et al., 2010) with *RICG^{fx/fx}* mice, and examined the effects of GFR α 1 ablation in GABAergic cell precursors on the complement of all the major types of OB interneurons. Efficient recombination Cre-mediated was verified by immunostaining of GFR α 1 in sections of the septal area of 7-week-old *Gad67^{CRE};RICG^{fx/fx}* and *RICG^{fx/fx}* mice (Fig. S1). At birth, *Gad67^{CRE};RICG^{fx/fx}* mice showed 20–30% reduction in TH, CB and CR positive cells (Fig. 3A,C). This difference was maintained in the 8-week-old OB of the mutants (Fig. 3B,D), indicating that loss of OB GABAergic interneurons cannot be compensated by newly generated interneurons during adulthood. Together, these data suggested that GFR α 1 regulates the development of OB GABAergic interneurons cell-autonomously in GABAergic precursors.

In order to more directly assess the possibility of non-cell-autonomous effects of GFR α 1 on the complement of OB GABAergic interneurons, we investigated the impact of GFR α 1 loss in OSNs and projection neurons. Primary olfactory axons have been implicated in regulating early neurogenesis in the OB (de Carlos et al., 1995; Gong and Shipley, 1995), and there is also evidence that OE activity can influence the proliferation of precursor cells in the SVZ (Ma et al., 2009; Mandairon et al., 2003). Likewise, glutamate input from excitatory neurons has been shown to affect OB interneuron function (Abraham et al., 2010). At 8 weeks of age, mice lacking GFR α 1 in OSNs (*γ 8TTA-TetO^{Cre};RICG^{fx/fx}*) displayed a reduction in mature, OMP-positive OSNs that was comparable to the losses that we previously reported in the global *Gfra1* knockout (Marks et al., 2012) (Fig. S2A,B).

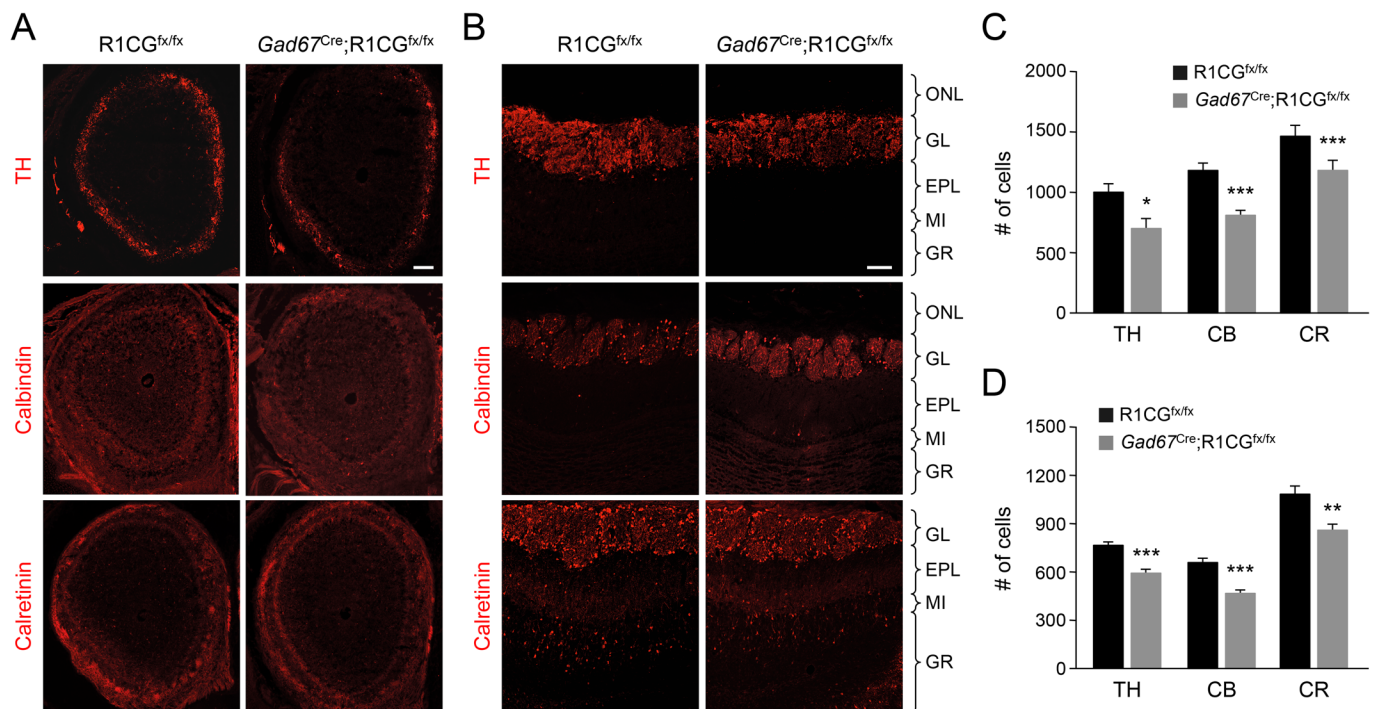


Fig. 3. Cell-autonomous loss of GABAergic interneurons in the OB of newborn and adult conditional GFR α 1 mutants. (A) Representative images of the OB of newborn *Gad67^{Cre};R1CG^{flox/flox}* conditional mutant and *R1CG^{flox/flox}* control mice immunostained for markers of OB GABAergic interneurons: tyrosine hydroxylase (TH), Calbindin and Calretinin. Scale bar: 100 μ m. (B) Representative images of the OB of P56 *Gad67^{Cre};R1CG^{flox/flox}* conditional mutant and *R1CG^{flox/flox}* control mice along the medial surface immunostained for markers of OB GABAergic interneurons: tyrosine hydroxylase (TH), Calbindin and Calretinin. Scale bar: 100 μ m. (C) Quantification of the number of cells expressing TH, Calbindin (CB) and Calretinin (CR) in the OB of newborn *Gad67^{Cre};R1CG^{flox/flox}* conditional mutants and *R1CG^{flox/flox}* control mice. The values represent total number of cells in fields encompassing the entire OB. $N=6$ mice per group; * $P<0.05$; *** $P<0.0005$. (D) Quantification of the number of cells expressing TH, Calbindin (CB) and Calretinin (CR) in the OB of P56 *Gad67^{Cre};R1CG^{flox/flox}* conditional mutants and *R1CG^{flox/flox}* control mice. The values represent number of cells counted in the glomerular layer of the medial surface of the OB (see the Materials and Methods for details). $N=6$ mice per group; ** $P<0.005$; *** $P<0.0005$. ONL, olfactory nerve layer; GL, glomerular layer; EPL, external plexiform layer; MI, mitral cell layer; GR, granule cell layer.

However, no reduction in GABAergic interneurons could be detected in either the newborn or adult OB of these mice (Fig. S3A,B). Similarly, mice lacking GFR α 1 in OB excitatory neurons (*Pcdh21^{Cre};R1CG^{flox/flox}*) also showed a normal complement of OB GABAergic interneurons at both ages (Fig. S3C,D). We note that no significant reduction in the numbers of either mitral or tufted cells could be detected in the OB of these mice (Fig. S4A–C), suggesting that the loss of OB excitatory neurons previously observed in the global knockout may be non-cell-autonomous and secondary to other defects in the olfactory system of those mice. In summary, together with our genetic fate mapping studies, these results support a cell-autonomous role for GFR α 1 in the regulation of OB GABAergic interneuron development.

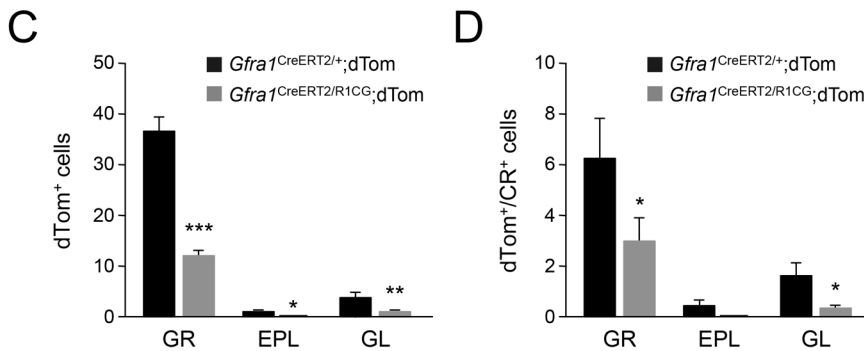
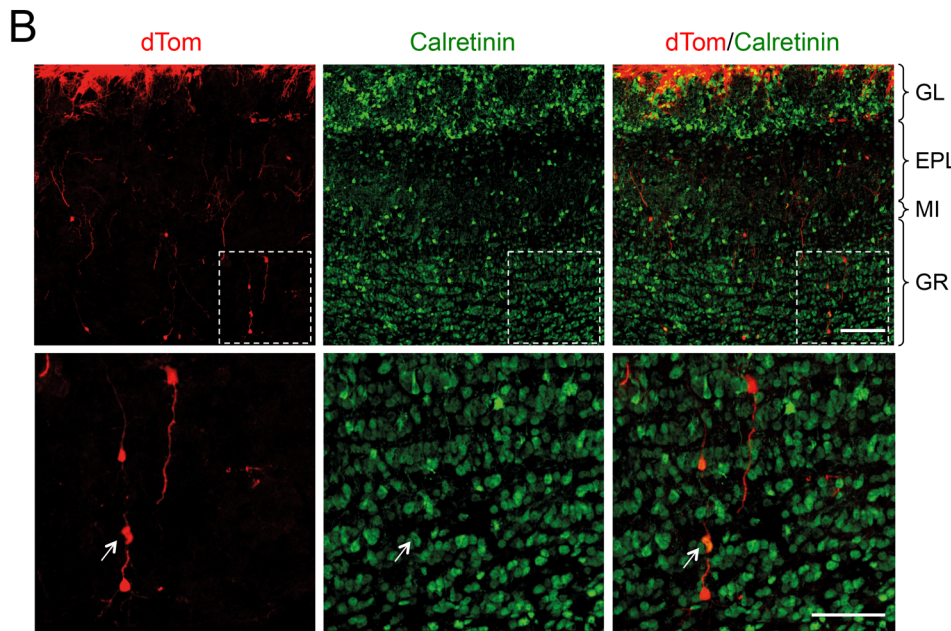
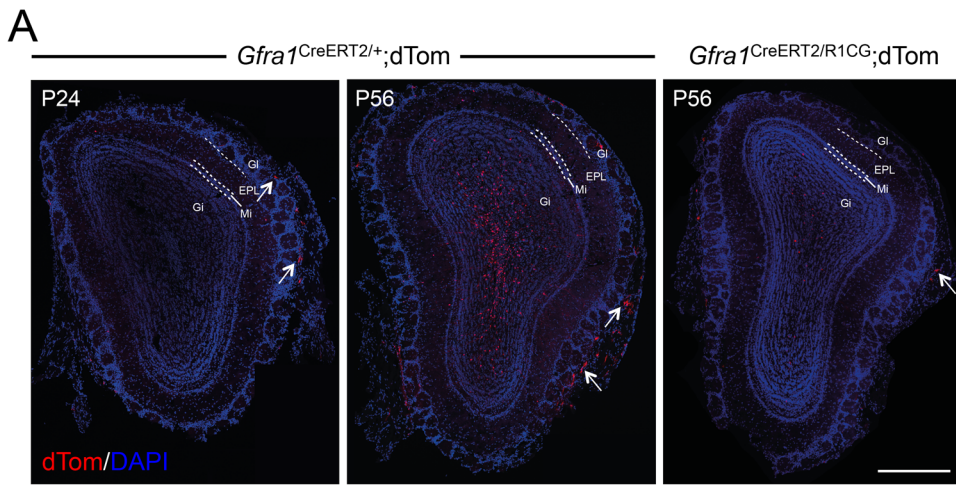
Continued requirement of GFR α 1 for the maintenance of the normal complement of OB interneurons in adult mice

Next, we investigated whether GFR α 1 is also required during postnatal stages for the maintenance of the normal complement of OB interneurons in the adult. To this end, we used the *Gfra1^{CreERT2/+}*;dTom mice (which are heterozygous for the wild-type *Gfra1* allele) during three consecutive days and assessed dTom-positive cells in the OB at P24 and at P56. At P24, one day after the last Tmx injection, a few labelled cells could be observed in the olfactory nerve layer, likely corresponding to ensheathing

cells [see Marks et al. (2012)], while no significant labelling could be detected in the GR or GL (Fig. 4A, left panel). At P56, on the other hand, numerous dTom-positive cells could be observed in the GL, and several labelled cells could also be seen in the glomerular layer and underlying external plexiform layer (Fig. 4A, centre panel). This is in agreement with observations indicating that SVZ neuroblasts take 3–4 weeks to reach the GL (Lemasson et al., 2005). Importantly, a significant loss of dTom-positive cells was seen across all layers in the OB of compound mutant *Gfra1^{CreERT2/R1CG};dTom* mice, which lost GFR α 1 expression from 3 weeks of age onwards after Tmx injection and Cre-mediated recombination (Fig. 4A, right panel). A quantitative analysis revealed prominent losses among CR-positive cells in the granule cell layer of these mice (Fig. 4B–D), which is the preferred fate adopted by postnatal neuroblasts (Lemasson et al., 2005; Batista-Brito et al., 2008).

Loss of GFR α 1 in OB GABAergic cell precursors affects neuroblast migration, differentiation and glial tunnel formation in the RMS

The loss of GABAergic interneurons in the OB of *Gad67^{Cre};R1CG^{flox/flox}* mice could be due to defects in proliferation or survival of GABAergic precursor cells, or in the migration or differentiation of RMS neuroblasts, all of which express GFR α 1. We assessed cell proliferation in the embryonic septum at the peak of OB interneuron generation (E16.5) and in the adult (P56) SVZ by BrdU injections. We did not detect any difference in the extent of BrdU incorporation between the mutants and the controls (Fig. S5).



We also quantified apoptotic cell death by staining for cleaved Caspase-3 combined with presence of pycnotic nuclei (assessed by DAPI staining) in conditional *GFRα1* mutants and control mice. We could not detect a significant increase in cell death at neurogenic sites, nor along the migratory pathway, nor in the OB in either newborn or adult (P56) conditional *GFRα1* mutant mice compared to controls (Fig. S6). Together, these results indicated that loss of *GFRα1* in GABAergic precursors does not affect their proliferation or survival.

Fig. 4. Continued requirement of *GFRα1* for the maintenance of the normal complement of OB interneurons in adult mice. (A) Representative coronal images of the OB of *Gfra1*^{CreERT2/+};dTom and *Gfra1*^{CreERT2/R1CG};dTom mice of the ages indicated after Tmx induced recombination at P21, P22 and P23. Arrows indicate ensheathing cells of the olfactory nerve layer. Scale bar: 500 μm. (B) Expression of dTom and Calretinin in the OB of P56 *Gfra1*^{CreERT2/+};dTom mice after Tmx induced recombination at P21, P22 and P23. Inserts in the second row show higher magnification of boxed areas. In four biological replicates, 20% of CR⁺ cells were also dTom⁺ (arrow). Scale bars: 50 μm (insets 25 μm). (C,D) Quantification of total (C) dTom-positive and (D) dTom/Calretinin double-positive cells in the OB of P56 *Gfra1*^{CreERT2/+};dTom and *Gfra1*^{CreERT2/R1CG};dTom mice after Tmx induced recombination at P21, P22 and P23. N=4 mice per group; **P*<0.05; ***P*<0.005; ****P*<0.0005. GL, glomerular layer; EPL, external plexiform layer; MI, mitral cell layer; IPL, internal plexiform layer; GR, granule cell layer.

Next, we turn our attention to the RMS of *Gad67*^{CRE};*R1CG*^{fx/fx} mice. At 8 weeks of age (P56), DCX staining of the RMS revealed a broader posterior RMS (pRMS) in the mutants (Fig. 5A,B). A similar phenotype has been reported in global knockouts of *Ncam* (Chazal et al., 2000); and was attributed to abnormal neuroblast migration in the RMS. As they leave the SVZ and enter the posterior RMS, neuroblasts accumulate in this region. In the *Ncam* mutants, the RMS enlargement is accompanied by an increase in GFAP-positive astroglial structures along the RMS, without a change in

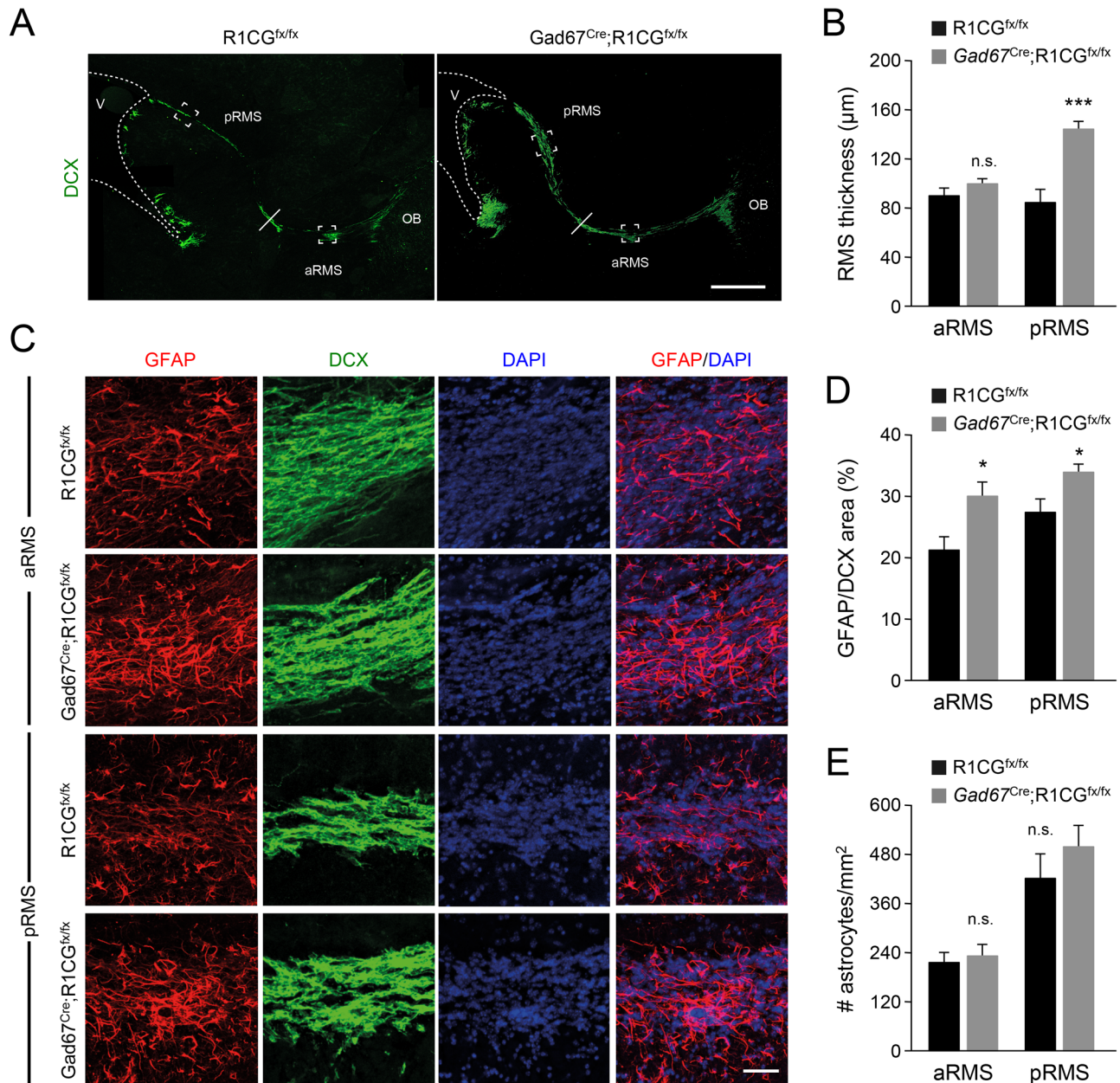


Fig. 5. RMS abnormalities in conditional mutant mice lacking *GFR α 1* in OB GABAergic cell precursors. (A) Representative images of DCX expression in a sagittal section of the RMS of P56 *Gad67^{Cre};^{flox/flox}* conditional mutant and *R1CG^{flox/flox}* control mice. The unbroken line marks the border between aRMS and pRMS. The ventricle (v) and OB are indicated. aRMS, anterior RMS; pRMS, posterior RMS. Scale bar: 500 μ m. (B) Quantification of aRMS and pRMS thickness at the positions boxed in panel A. $N=8$ mice per group. n.s., not significantly different; *** $P<0.0005$. (C) GFAP (red), DCX (green) and DAPI (blue) staining of sagittal sections through the anterior (aRMS) and posterior (pRMS) RMS of P56 *Gad67^{Cre};^{flox/flox}* conditional mutant and *R1CG^{flox/flox}* control mice. Scale bar: 25 μ m. (D) Percentage of DCX area covered by GFAP-positive astroglial structures in the aRMS and pRMS of P56 *Gad67^{Cre};^{flox/flox}* conditional mutant and *R1CG^{flox/flox}* control mice. $N=8$ mice per group; * $P<0.05$. (E) Quantification of astrocyte number per unit of DCX⁺ area (assessed by DAPI nuclei within GFAP⁺ structures) in the aRMS and pRMS of P56 *Gad67^{Cre};^{flox/flox}* conditional mutant and *R1CG^{flox/flox}* control mice. $N=8$ mice per group. n.s., not significantly different.

astrocyte proliferation or number (Chazal et al., 2000). Astrocytes ensheathing the RMS are thought to provide guidance to migrating RMS neuroblasts (Alvarez-Buylla and Lim, 2004). We assessed astroglial coverage in the RMS of *Gad67^{CRE};^{flox/flox}* mice by quantifying the area covered by GFAP immunostaining within the region stained by DCX in anterior and posterior RMS regions. We detected a significant increase in the mutants compared to controls (Fig. 5C,D) without a change in astrocyte number (Fig. 6E), suggesting enlarge astrocyte area in the RMS of the mutants. In addition, the RMS of *Gad67^{CRE};^{flox/flox}* mice showed an

increased number of CR expressing cells relative to DCX-positive area (Fig. 6A,B), suggesting premature differentiation of RMS neuroblasts in the mutant, a phenotype that has also been observed in *Ncam* deficient mice (Röckle and Hildebrandt, 2016).

In order to investigate neuroblast migration in the RMS, we used *in vivo* electroporation to introduce a fluorescent reporter (RFP) together with Cre recombinase in the ventricular zone of newborn *R1CG^{flox/flox}* mice. This method resulted in efficient electroporation of GFAP-positive type B stem cells and *Ascl1*/MASH1-positive type C transit amplifying cells in the SVZ (Fig. S7A,B).

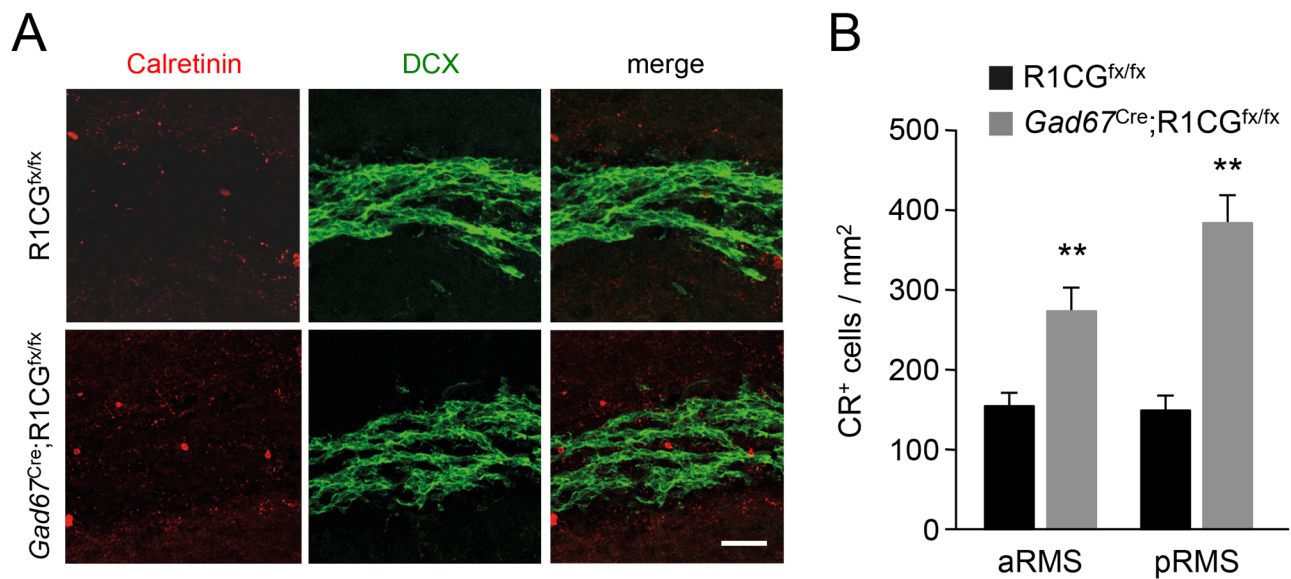


Fig. 6. Premature differentiation of RMS neuroblasts in conditional mutant mice lacking $GFR\alpha 1$ in OB GABAergic cell precursors.

(A) Immunostaining for Calretinin (red) and DCX (green) in the posterior RMS of P56 *Gad67^{Cre};R1CG^{fx/fx}* conditional mutant and *R1CG^{fx/fx}* control mice. Scale bar: 50 μ m. (B) Quantification of Calretinin positive cells per unit DCX⁺ area in the RMS of P56 *Gad67^{Cre};R1CG^{fx/fx}* conditional mutant and *R1CG^{fx/fx}* control mice. $N=6$ mice per group. ** $P<0.005$.

At 3 weeks of age (P21), *R1CG^{fx/fx}* neuroblasts that had undergone Cre-mediated recombination (i.e. double-positive for RFP and PSA-NCAM) accumulated in the posterior RMS to a larger extent than in controls that did not receive Cre (Fig. 7A,B), indicating a slower migration along the RMS after loss of $GFR\alpha 1$ expression. We also measured the angle between the leading process of individual, electroporated neuroblasts and the main direction of the RMS (see the Materials and Methods section). We found that Cre-mediated loss of $GFR\alpha 1$ significantly increased the angle of the leading process in migrating neuroblasts in the RMS (Fig. 8C,D), in agreement with abnormal migratory behaviour. Together, these results indicate altered neuroblast migration, premature differentiation and abnormal glial tunnel formation in the RMS of mice lacking $GFR\alpha 1$ in OB GABAergic cell precursors.

DISCUSSION

In the present study, we have shown that $GFR\alpha 1$ is expressed in GABAergic precursors contributing to all classes of OB interneurons and that conditional loss of $GFR\alpha 1$ in GABAergic cells, during development or in adulthood, results in reduced numbers of all major OB interneurons subtypes. In addition, the RMS of conditional mutants shows abnormal neuroblast migration, differentiation and increased astroglial reactivity. These results indicate a cell-autonomous requirement of $GFR\alpha 1$ in the cell lineage that gives rise to OB interneurons.

OB interneurons are thought to be mainly generated in the LGE and septum from E14.5 onwards during embryonic development (Pencea and Luskin, 2003; Wichterle et al., 2001). It has also been reported that some OB interneurons may be generated in the olfactory primordium from E11 (Hinds, 1968; Vergaño-Vera et al., 2006). We have detected expression of $GFR\alpha 1$ in subpopulations of cells in the septum, olfactory primordium and developing OB, but not in the LGE, of E12.5 embryos. Some of those cells also expressed Sp8, a known marker of the precursors of OB CR-positive cells. These observations suggest a significant level of heterogeneity among precursors of OB GABAergic interneurons from early stages of embryonic development. In the adult,

interneurons destined for the OB originate from the SVZ, and the majority of those cells differentiate into granule cells (Lemasson et al., 2005; Batista-Brito et al., 2008). This is in agreement with our observation that the majority of OB interneurons deriving from $GFR\alpha 1$ -expressing SVZ precursors become CR-positive cells of the granule cell layer. Depending on their location, granule cells can differ in their connectivity and functional properties (Merkle et al., 2014). The fact that granule cells derived from $GFR\alpha 1^+$ precursors appeared distributed across superficial, intermediate and deep layers of the GL suggests that they are themselves functionally heterogeneous. The expression of $GFR\alpha 1$ in migratory precursors, but not in mature OB GABAergic interneurons, indicates that this receptor is downregulated during the final maturation of these cells. Transient expression of $GFR\alpha 1$ by migratory precursors of GABAergic neurons seems to be a common property of this type of cell as it has also been observed in GABAergic precursors of the MGE that give rise to cortical interneurons (Canty et al., 2009; Pozas and Ibáñez, 2005), immature molecular layer interneurons of the cerebellum (Sergaki et al., 2017) and in migratory precursors of Purkinje cells (Sergaki and Ibáñez, 2017). It remains unclear why or how GABAergic precursor cells downregulate expression of $GFR\alpha 1$ as they develop, but it may be related to their cessation of cell migration and incorporation into mature neuronal circuits.

The extent of the loss of GABAergic interneurons in the OB of newborn and adult *Gad67^{Cre};R1CG^{fx/fx}* mutant mice (approximately 20–30%) was comparable to that previously observed in global *Gfral* knockout mice (Marks et al., 2012). Interestingly, the loss of mature OSNs observed in $\gamma 8TTA-TetO^{Cre};R1CG^{fx/fx}$ mice was not accompanied by a reduction in OB GABAergic interneurons in these mutants. Thus, although OE activity has been shown to influence early OB neurogenesis (de Carlos et al., 1995; Gong and Shipley, 1995), there does not seem to be a simple relationship between the complements of OSN and OB interneurons. Finally, removal of $GFR\alpha 1$ in mitral and tufted cells did not affect the number of GABAergic neurons in the OB. Together, these results support a cell-autonomous function for $GFR\alpha 1$ in the GABAergic cell lineage that gives rise to OB interneurons.

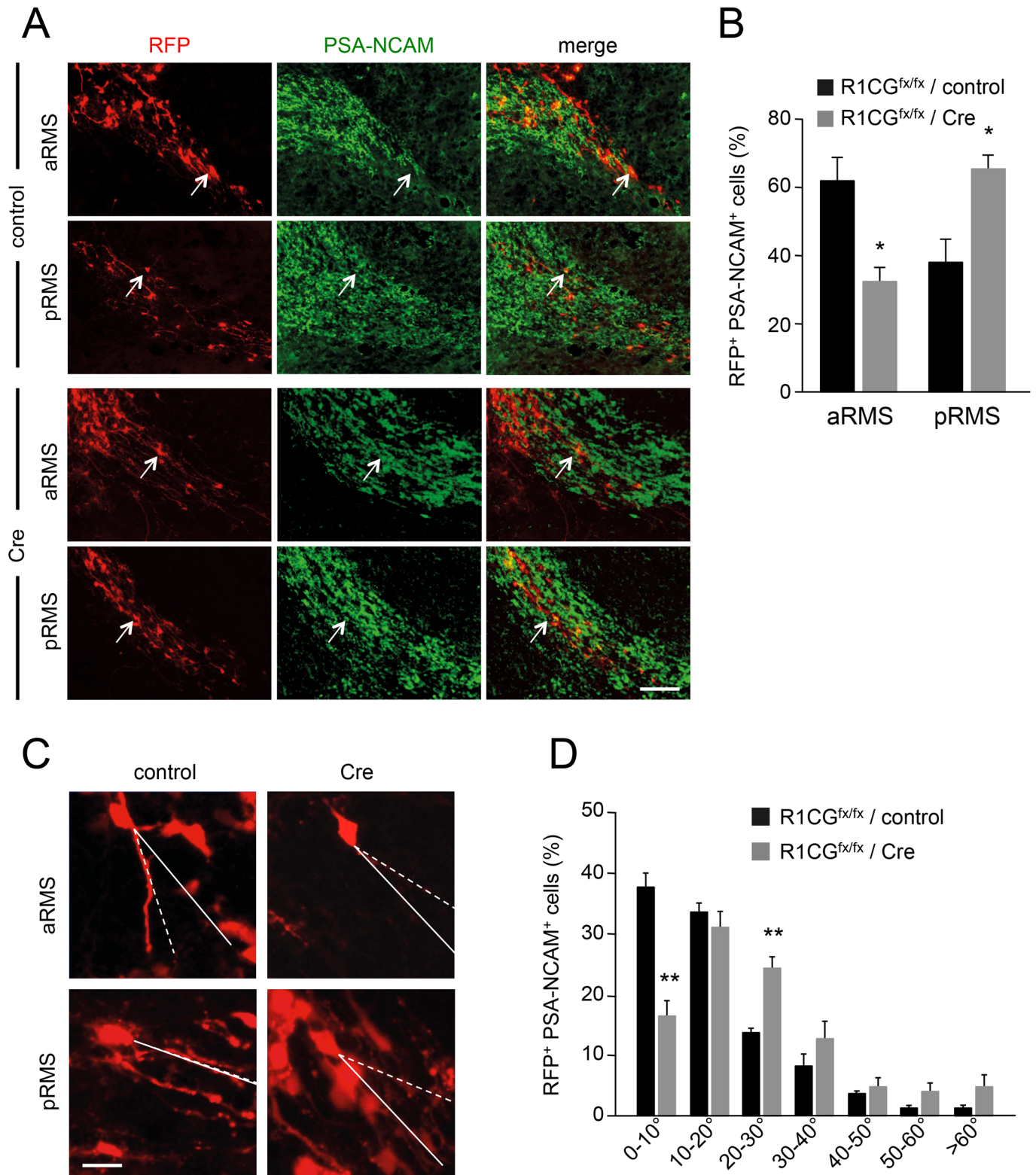


Fig. 7. See next page for legend.

Together with RET, GFR α 1 has been shown to contribute to GDNF-mediated cell survival. Among GABAergic cells, for example, we have recently reported that cerebellar molecular layer interneurons depend upon expression of GFR α 1 and RET during development for their survival in response to GDNF derived from Purkinje cells (Sergaki et al., 2017). In cells that do not express RET,

GFR α 1 has been implicated in cell migration, either in partnership with NCAM, as in the case of Purkinje cell precursors (Sergaki and Ibáñez, 2017), or together with other yet unknown receptors, as in the GABAergic precursors derived from the MGE (Perrinjaquet et al., 2011; Pozas and Ibáñez, 2005). In this study, we have shown that the specific loss of GFR α 1 in GABAergic cells does not alter

Fig. 7. Abnormal neuroblast migration in the RMS of conditional mutant mice lacking *GFR α 1* in OB GABAergic cell precursors.

(A) Representative images of RFP (red, marking all electroporated cells) and PSA-NCAM (green, marking RMS neuroblasts) expression in the anterior and posterior RMS of P21 *R1CG^{fx/fx}* mice after ventricular electroporation of Cre-expressing or control plasmids at P0. Arrows indicate double-positive cells. Scale bar: 50 μ m. (B) Quantification of the proportion of RFP/PSA-NCAM double-positive cells in the anterior and posterior RMS of P21 *R1CG^{fx/fx}* mice after ventricular electroporation of Cre-expressing or control plasmids normalised to the total number of double-positive cells in the RMS. $N=7$ mice per group. * $P<0.05$. (C) Representative images of RFP⁺ cells in the anterior and posterior RMS of P21 *R1CG^{fx/fx}* mice after ventricular electroporation of Cre-expressing or control plasmids at P0. The angles between the leading process of individual, electroporated neuroblasts (dashed lines) and the main direction of the RMS (solid lines) are indicated. Scale bar: 10 μ m. (D) Analysis of the angle of the leading process with respect to the lateral walls of the RMS (as defined by PSA-NCMA staining) in RFP/PSA-NCAM double-positive cells of the RMS of P21 *R1CG^{fx/fx}* mice after ventricular electroporation of Cre-expressing or control plasmids. The analysis included both anterior and posterior RMS. $N=4$ (control); $N=7$ (Cre) mice per group. $P=**$, <0.005 .

their proliferation or survival in neurogenic areas known to give rise to OB GABAergic interneurons, namely the embryonic septum and adult SVZ. On the other hand, we have presented several lines of evidence that indicate a role for *GFR α 1* in the migration and early differentiation of these cells. First, the posterior RMS of conditional mutants lacking *GFR α 1* in GABAergic cells is enlarged, a phenotype that has also been described in mice lacking NCAM (Chazal et al., 2000) and which is thought to result from aberrant migration of these cells in the initial segments of the RMS. Second, *GFR α 1*-expressing SVZ precursors labelled by Cre-mediated recombination at their site of origin also accumulate in the posterior RMS at the expense of more distal RMS regions, in agreement with a sluggish migratory behaviour. Finally, a proportion of RMS neuroblast in *Gad67^{CRE}*; *R1CG^{fx/fx}* mice prematurely differentiated into CR-positive neurons, a phenotype that has also been observed in *Ncam* knockouts (Röckle and Hildebrandt, 2016), and which suggests that *GFR α 1* may contribute to maintain GABAergic neuroblasts in an immature, migration-prone state. In addition, we observed increased astrocyte area in the RMS of *Gad67^{CRE}*; *R1CG^{fx/fx}* mice, suggesting astrocyte activation (a.k.a. astrogliosis by some authors), which has also been reported in *Ncam* mutants (Chazal et al., 2000). As RMS astrocytes do not express *GFR α 1*, this reaction may be an indirect consequence of the abnormal behaviour of RMS neuroblasts in mutant mice lacking *GFR α 1* in GABAergic cells, and suggest a close interplay between RMS astrocytes and migrating neuroblasts. Although astrocytes are only generated later in development, radial glial cells may be playing a similar scaffold role for early GABAergic cells destined to the OB during embryonic development (Alves et al., 2002).

In summary, our results indicate that transient expression of *GFR α 1* in OB interneuron precursors plays important roles in a cell-autonomous fashion during development as well as adulthood, thus resolving the unexplained phenotype previously reported in global *Gfral* mutants. Although the similarities with the phenotypes described in mice lacking NCAM suggest that this cell adhesion molecule serves as *GFR α 1* co-receptor in the murine RMS, the precise mechanisms by which *GFR α 1* regulates the migration of neuroblasts to the OB needs further investigation.

MATERIALS AND METHODS

Animals

The mouse lines utilised in this study have been described previously and are as follows: (i) conditional *Gfral* mutants, referred to as *R1CG^{fx/fx}*, express GFP from the *Gfral* locus after Cre-mediated recombination

(Uesaka et al., 2007); (ii) *Gad67^{Cre}* (Tolu et al., 2010); (iii) *γ 8TTA-tetO^{Cre}* (Nguyen et al., 2007); (iv) *Pcdh21^{Cre}* (Nagai et al., 2005); (v) *EIIa^{Cre}* (Lakso et al., 1996); (vi) *ROSA26^{dTom}* (Madisen et al., 2010); (vii) *Gad^{GFP}* (Tamamaki et al., 2003); and (viii) *Gfral^{CreERT2}* (Sergaki and Ibáñez, 2017). All mouse lines were bred on a C57BL6 background. Both males and females were used for these studies. The day of the vaginal plug was considered as embryonic day 0.5 (E0.5). Animal protocols were approved by Stockholm's Norra Djurförsöksetiska Nämnd and are in accordance with the ethical guidelines of the Karolinska Institute.

Immunohistochemistry and *in situ* hybridization

Embryos and neonatal pups were decapitated and fixed in 4% paraformaldehyde (PFA, Sigma-Aldrich) for 24 h at 4°C. Three- or 8-week-old mice were deeply anaesthetised with isoflurane, and perfused transcardially with ice-cold PBS followed by 4% PFA. All samples were subsequently washed in PBS, cryoprotected in 30% sucrose at 4°C and serially sectioned (12 μ m) on a cryostat (Cryostar, NX70, Microm, Bicester, UK). After blocking in 5% serum for 1 h, sections were incubated in the following primary antibodies overnight at room temperature (RT): rabbit anti-CB (D28K, ab1778, Millipore, 1:500), rabbit anti-CR (ab5054, Millipore, 1:500), rabbit anti-TH (ab657012, Millipore, 1:500), chicken anti-GFP (ab13970, Abcam, 1:500), goat anti-GFP (ab6673, Abcam, 1:500), rabbit anti-cleaved Caspase-3 (Asp175, 9661, Cell Signaling Technology, 1:500), guinea pig anti-doublecortin (DCX, ab2253, Millipore, 1:500), goat anti-Sp8 (C18, sc104661, Santa Cruz Biotechnology, 1:500), anti-mouse anti-PSA-NCAM (clone 2-2B, MAB5324, Millipore, 1:500), rabbit anti-GFAP (ab5804, Millipore, 1:500), rabbit anti-ER81 (ab36788-50, Abcam, 1:500), goat anti-OMP (Wako Pure Chemicals, Richmond, USA, 1:500), rabbit anti-GAP43 (Novus Biochemicals, Littleton, USA, 1:500), rabbit anti-Ascl1/MASH1 (ab74065, Abcam, 1:1000), mouse anti-Reelin (MAB5364, Millipore, 1:500), and rat anti-BrdU (347580, AbD Serotec, Hercules, USA, 1:500). After three washes in PBS, slides were incubated with fluorescently labelled secondary antibodies (Jackson ImmunoResearch, 1:500) for 2 h at RT. Slides were then washed in PBS, counterstained with 4'-6-diamidino-2-phenylindole (DAPI) and coverslipped in fluorescent mounting medium (Dako, Glostrup, Denmark). For *in situ* hybridization, a fragment corresponding to the extracellular domain of mouse *GFR α 1* was amplified by RT-PCR and subcloned by TOPO-TA cloning (Invitrogen). Non-radioactive fluorescent *in situ* hybridization was performed by hybridization overnight at 58°C using a specific antisense riboprobe labelled with biotin-dUTP (Roche Diagnostics, Basel, Switzerland). Sections were processed using tyramide signal amplification (Perkin Elmer, Waltham, USA). Finally, sections were developed with Streptavidin 488 (Millipore, 1:500). Control hybridizations with sense riboprobe did not give any signal (Pozas and Ibáñez, 2005).

BrdU labelling and Tamoxifen injection

Adult (2-months-old) and E16.5 pregnant animals were injected intraperitoneally with BrdU (100 mg/kg body weight, Sigma-Aldrich) in PBS. After 1 h (adult mice) or 30 min (E16.5) the mice were deeply anaesthetised and perfused transcardially with PBS followed by 4% PFA. Brains were removed, postfixed, cryoprotected and cut as described above. Sections were incubated in 1 M HCl at 45°C for 45 min to denature the DNA before immunohistochemical staining. For tamoxifen administration, time-mated pregnant females were injected intraperitoneally with Tamoxifen (Sigma-Aldrich, T5648) in corn oil at a concentration of 100 mg/kg body weight.

Electroporation of newborn mouse pups

Electroporation of the ventricle wall in neuronal mouse pups was performed as described (Chesler et al., 2008) after intraventricular injection of plasmids encoding red-fluorescent protein (RFP) with or without a Cre recombinase-encoding plasmid, combined with 0.05% Fast Green (Sigma-Aldrich) as a tracer. Briefly, neonatal pups were shortly anaesthetised by hypothermia and 1–2 μ l plasmid solution was injected into each lateral ventricle. Tweezer electrodes were placed horizontally as well as tilted in a 45° angle to each side. A square wave electroporator NEPA21 (Nepagene, Chiba, Japan) was

used to deliver 2×10 ms pulses of 175 V for electroporation followed by 3×50 ms pulses of 15 V for transfer (with 50 ms intervals). Three weeks later, the mice were perfused, postfixed and processed for immunohistochemistry as described above.

Image analysis

Immunofluorescence images were captured with a Carl Zeiss LSM710 confocal microscope (10 μm thick, 20× magnification, z=10). For interneuron counts in the OB, nine representative images were sampled from the anterior, middle and posterior sagittal planes of the OB for each animal within each group. For OB cell counts in newborn mice, confocal images were collected encompassing the entire OB in coronal view. In 8-week-old mice, cells within the glomerular layer of the medial portion of the OB were counted in a 533×533 μm frame. For the SVZ, cells were counted in a 533×187 μm frame in sections immunostained for BrdU. Cells were manually counted using ImageJ software and summed across the nine images per OB for statistical comparison between animals. The aRMS was defined as the DCX positive area between the OB and the bend between the horizontal and vertical limb of the RMS, whereas the pRMS was defined as the DCX positive area between this bend and the SVZ. Thickness measurements were carried out in a 100 μm distance from the SVZ for the pRMS and a 500 μm distance from the OB for the aRMS. GFAP area measurements in the RMS were done relative to the area covered by DCX staining and results are given as percentage of DCX-positive area. Analysis of the angle of migration in electroporated cells was performed using ZEN software (ZEN Blue Edition, Zeiss, Jena, Germany). A straight line parallel to the RMS main direction, as defined by PSA-NCAM staining, was drawn and the angle between this line and the vector of the cellular leading process was measured for each electroporated (i.e. RFP⁺) cell.

Statistical analyses

Statistical analysis were made with Prism 5 (GraphPad Inc., La Jolla, USA). Values in all graphs are shown as means±standard error of the mean (s.e.m.). Student's *t*-test and ANOVA were used to test statistical significance, assuming a two-tailed distribution and two-sample unequal variance. A *P*-value below of 0.05 was considered as statistically significant.

Acknowledgements

We thank Hideki Enomoto, Hannah Monyer, Stephan Teglund and Leonardo Belluscio for providing mutant mice, Masanori Uchikawa for the RFP-plasmid and Annika Andersson and Wei Wang for technical assistance.

Competing interests

The authors declare no competing or financial interests.

Author contributions

S.Z. and C.F.I. planned the experiments. S.Z. and D.F.S. performed the experiments. S.Z. prepared the figures. C.F.I. wrote the manuscript.

Funding

Support for this research was provided by grants to C.F.I. from the Swedish Research Council, Swedish Cancer Society, Knut and Alice Wallenbergs Foundation (Wallenberg Scholars Program), Strategic Research Program in Regenerative Medicine KI, and National University of Singapore; and from Wenner-Gren Foundation, to S.Z.

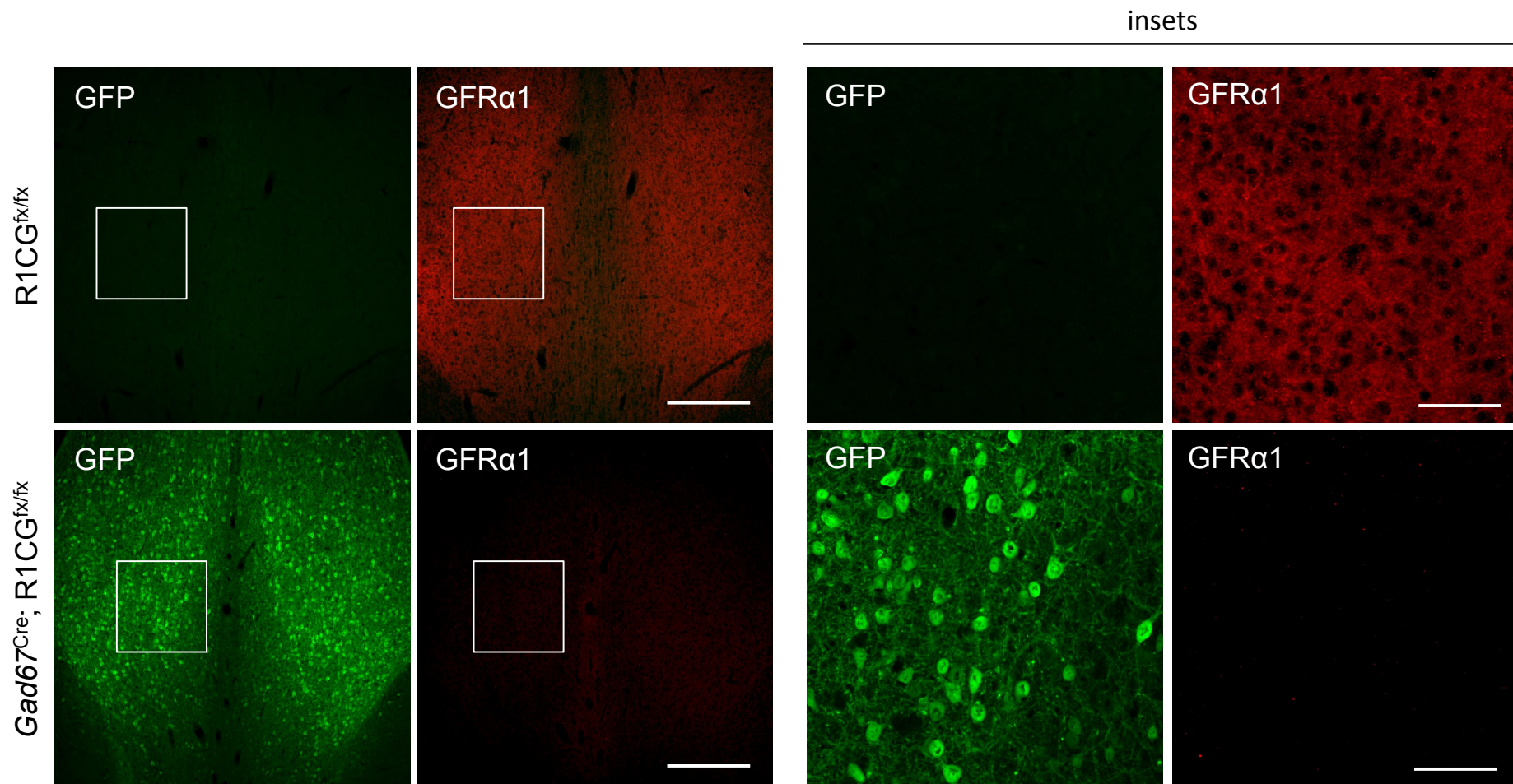
Supplementary information

Supplementary information available online at <http://bio.biologists.org/lookup/doi/10.1242/bio.033753.supplemental>

References

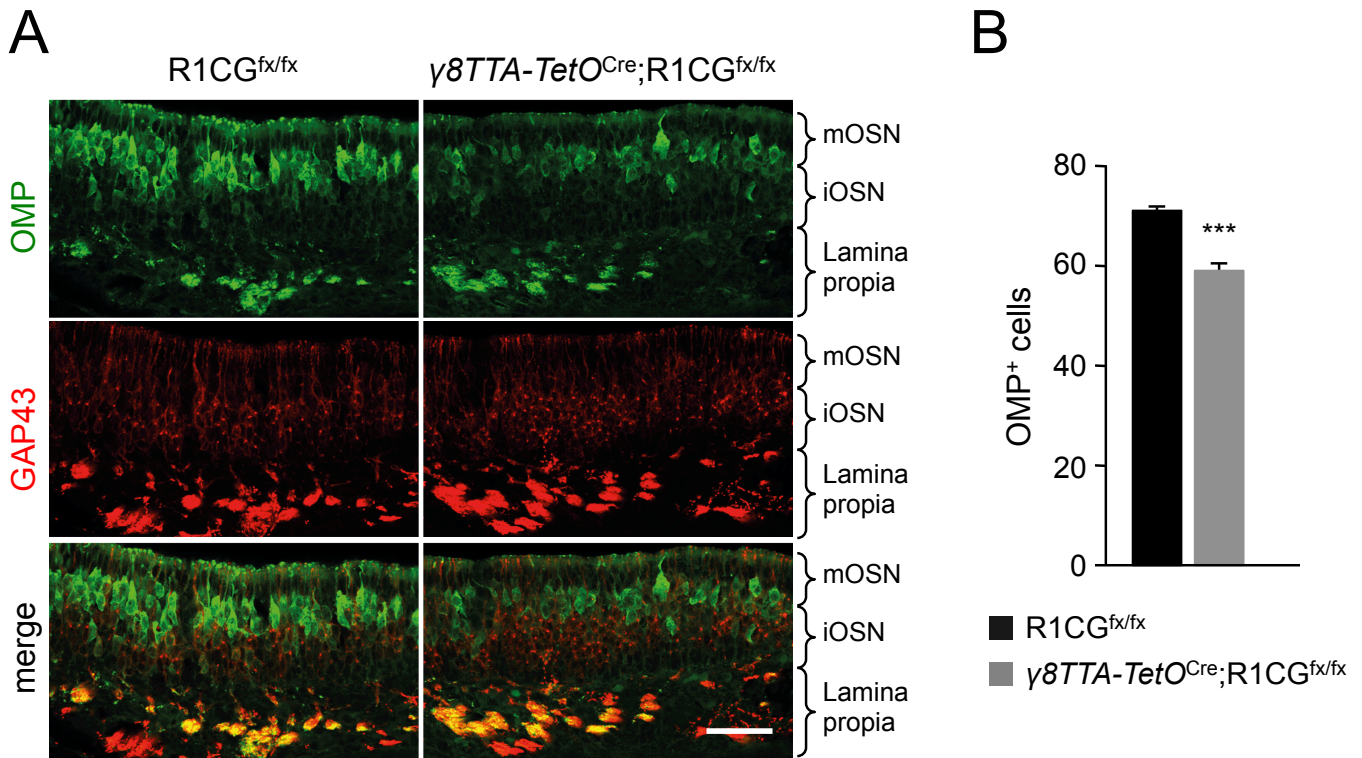
- Abraham, N. M., Egger, V., Shimshek, D. R., Renden, R., Fukunaga, I., Sprengel, R., Seeburg, P. H., Klugmann, M., Margrie, T. W., Schaefer, A. T. et al. (2010). Synaptic inhibition in the olfactory bulb accelerates odor discrimination in mice. *Neuron* **65**, 399-411.
- Altman, J. (1969). Autoradiographic and histological studies of postnatal neurogenesis. IV. Cell proliferation and migration in the anterior forebrain, with special reference to persisting neurogenesis in the olfactory bulb. *The Journal of Comparative Neurology* **137**, 433-457.
- Alvarez-Buylla, A. and Lim, D. A. (2004). For the long run: maintaining germinal niches in the adult brain. *Neuron* **41**, 683-686.
- Alves, J. A. J., Barone, P., Engelder, S., Fróes, M. M. and Menezes, J. R. L. (2002). Initial stages of radial glia astrocytic transformation in the early postnatal anterior subventricular zone. *J. Neurobiol.* **52**, 251-265.
- Azim, K., Fiorelli, R., Zweifel, S., Hurtado-Chong, A., Yoshikawa, K., Slomianka, L. and Raineteau, O. (2012). 3-dimensional examination of the adult mouse subventricular zone reveals lineage-specific microdomains. *PLoS ONE* **7**, e49087.
- Batista-Brito, R., Close, J., Machold, R. and Fishell, G. (2008). The distinct temporal origins of olfactory bulb interneuron subtypes. *J. Neurosci.* **28**, 3966-3975.
- Canty, A. J., Dietze, J., Harvey, M., Enomoto, H., Milbrandt, J. and Ibáñez, C. F. (2009). Regionalized loss of parvalbumin interneurons in the cerebral cortex of mice with deficits in GFRalpha1 signaling. *J. Neurosci.* **29**, 10695-10705.
- Chazal, G., Durbec, P., Jankovski, A., Rougon, G. and Cremer, H. (2000). Consequences of neural cell adhesion molecule deficiency on cell migration in the rostral migratory stream of the mouse. *J. Neurosci.* **20**, 1446-1457.
- Chesler, A. T., Le Pichon, C. E., Brann, J. H., Araneda, R. C., Zou, D.-J. and Firestein, S. (2008). Selective gene expression by postnatal electroporation during olfactory interneuron neurogenesis. *PLoS ONE* **3**, e1517.
- de Carlos, J. A., López-Mascaraque, L. and Valverde, F. (1995). The telencephalic vesicles are innervated by olfactory placode-derived cells: a possible mechanism to induce neocortical development. *Neuroscience* **68**, 1167-1178.
- Fuentealba, L. C., Rompani, S. B., Parraguez, J. I., Obner, K., Romero, R., Cepko, C. L. and Alvarez-Buylla, A. (2015). Embryonic origin of postnatal neural stem cells. *Cell* **161**, 1644-1655.
- Gong, Q. and Shipley, M. T. (1995). Evidence that pioneer olfactory axons regulate telencephalon cell cycle kinetics to induce the formation of the olfactory bulb. *Neuron* **14**, 91-101.
- Hinds, J. W. (1968). Autoradiographic study of histogenesis in the mouse olfactory bulb. II. Cell proliferation and migration. *The Journal of Comparative Neurology* **134**, 305-322.
- Kosaka, K. and Kosaka, T. (2007). Chemical properties of type 1 and type 2 periglomerular cells in the mouse olfactory bulb are different from those in the rat olfactory bulb. *Brain Res.* **1167**, 42-55.
- Lakso, M., Pichel, J. G., Gorman, J. R., Sauer, B., Okamoto, Y., Lee, E., Alt, F. W. and Westphal, H. (1996). Efficient in vivo manipulation of mouse genomic sequences at the zygote stage. *Proc. Natl. Acad. Sci. USA* **93**, 5860-5865.
- Lledo, P.-M., Alonso, M. and Grubb, M. S. (2006). Adult neurogenesis and functional plasticity in neuronal circuits **7**, 179-193.
- Lemasson, M., Saghatelian, A., Olivo-Marin, J.-C. and Lledo, P.-M. (2005). Neonatal and adult neurogenesis provide two distinct populations of newborn neurons to the mouse olfactory bulb. *J. Neurosci.* **25**, 6816-6825.
- Lin, L. F., Doherty, D. H., Lile, J. D., Bektesh, S. and Collins, F. (1993). GDNF: a glial cell line-derived neurotrophic factor for midbrain dopaminergic neurons. *Science* **260**, 1130-1132.
- Lois, C. and Alvarez-Buylla, A. (1994). Long-distance neuronal migration in the adult mammalian brain. *Science* **264**, 1145-1148.
- Luskin, M. B. (1993). Restricted proliferation and migration of postnatally generated neurons derived from the forebrain subventricular zone. *Neuron* **11**, 173-189.
- Luskin, M. B. (1998). Neuroblasts of the postnatal mammalian forebrain: their phenotype and fate. *J. Neurobiol.* **36**, 221-233.
- Ma, D. K., Kim, W. R., Ming, G.-L. and Song, H. (2009). Activity-dependent extrinsic regulation of adult olfactory bulb and hippocampal neurogenesis. *Ann. N. Y. Acad. Sci.* **1170**, 664-673.
- Madisen, L., Zwingman, T. A., Sunkin, S. M., Oh, S. W., Zariwala, H. A., Gu, H., Ng, L. L., Palmiter, R. D., Hawrylycz, M. J., Jones, A. R. et al. (2010). A robust and high-throughput Cre reporting and characterization system for the whole mouse brain. *Nat. Neurosci.* **13**, 133-140.
- Mandairon, N., Jourdan, F. and Didier, A. (2003). Deprivation of sensory inputs to the olfactory bulb up-regulates cell death and proliferation in the subventricular zone of adult mice. *Neuroscience* **119**, 507-516.
- Marks, C., Belluscio, L. and Ibáñez, C. F. (2012). Critical role of GFRα1 in the development and function of the main olfactory system. *J. Neurosci.* **32**, 17306-17320.
- Merkle, F. T., Mirzadeh, Z. and Alvarez-Buylla, A. (2007). Mosaic organization of neural stem cells in the adult brain. *Science* **317**, 381-384.
- Merkle, F. T., Fuentealba, L. C., Sanders, T. A., Magno, L., Kessar, N. and Alvarez-Buylla, A. (2014). Adult neural stem cells in distinct microdomains generate previously unknown interneuron types. *Nat. Neurosci.* **17**, 207-214.
- Nagai, Y., Sano, H. and Yokoi, M. (2005). Transgenic expression of Cre recombinase in mitral/tufted cells of the olfactory bulb. *Jb. wiss. Bot.* **43**, 12-16.
- Nguyen, M. Q., Zhou, Z., Marks, C. A., Ryba, N. J. P. and Belluscio, L. (2007). Prominent roles for odorant receptor coding sequences in allelic exclusion. *Cell* **131**, 1009-1017.
- Paratcha, G., Ledda, F. and Ibáñez, C. F. (2003). The neural cell adhesion molecule NCAM is an alternative signaling receptor for GDNF family ligands. *Cell* **113**, 867-879.

- Paratcha, G., Ibáñez, C. F. and Ledda, F. (2006). GDNF is a chemoattractant factor for neuronal precursor cells in the rostral migratory stream. *Mol. Cell. Neurosci.* **31**, 505-514.
- Pencea, V. and Luskin, M. B. (2003). Prenatal development of the rodent rostral migratory stream. *J. Comp. Neurol.* **463**, 402-418.
- Perrinjaquet, M., Sjöstrand, D., Moliner, A., Zechel, S., Lamballe, F., Maina, F. and Ibáñez, C. F. (2011). MET signaling in GABAergic neuronal precursors of the medial ganglionic eminence restricts GDNF activity in cells that express GFR α 1 and a new transmembrane receptor partner. *J. Cell Sci.* **124**, 2797-2805.
- Pozas, E. and Ibáñez, C. F. (2005). GDNF and GFR α 1 promote differentiation and tangential migration of cortical GABAergic neurons. *Neuron* **45**, 701-713.
- Qin, S., Ware, S. M., Waclaw, R. R. and Campbell, K. (2017). Septal contributions to olfactory bulb interneuron diversity in the embryonic mouse telencephalon: role of the homeobox gene Gsx2. *Neural Development* **12**, 13.
- Röckle, I. and Hildebrandt, H. (2016). Deficits of olfactory interneurons in polysialyltransferase- and NCAM-deficient mice. *Dev. Neurobiol.* **76**, 421-433.
- Sawada, M., Kaneko, N., Inada, H., Wake, H., Kato, Y., Yanagawa, Y., Kobayashi, K., Nemoto, T., Nabekura, J. and Sawamoto, K. (2011). Sensory input regulates spatial and subtype-specific patterns of neuronal turnover in the adult olfactory bulb. *J. Neurosci.* **31**, 11587-11596.
- Sergaki, M. C. and Ibáñez, C. F. (2017). GFR α 1 regulates Purkinje cell migration by counteracting NCAM function. *Cell Rep.* **18**, 367-379.
- Sergaki, M. C., López-Ramos, J. C., Stagkourakis, S., Gruart, A., Broberger, C., Delgado-García, J. M. and Ibáñez, C. F. (2017). Compromised survival of cerebellar molecular layer interneurons lacking GDNF receptors GFR α 1 or RET impairs normal cerebellar motor learning. *Cell Rep.* **19**, 1977-1986.
- Tamamaki, N., Yanagawa, Y., Tomioka, R., Miyazaki, J.-I., Obata, K. and Kaneko, T. (2003). Green fluorescent protein expression and colocalization with calretinin, parvalbumin, and somatostatin in the GAD67-GFP knock-in mouse. *J. Comp. Neurol.* **467**, 60-79.
- Tolu, S., Avale, M. E., Nakatani, H., Pons, S., Parnaudeau, S., Tronche, F., Vogt, A., Monyer, H., Vogel, R., de Chaumont, F. et al. (2010). A versatile system for the neuronal subtype specific expression of lentiviral vectors. *FASEB J.* **24**, 723-730.
- Treanor, J. J. S., Goodman, L., de Sauvage, F., Stone, D. M., Poulsen, K. T., Beck, C. D., Gray, C., Armanini, M. P., Pollock, R. A., Hefti, F. et al. (1996). Characterization of a multicomponent receptor for GDNF. *Nature* **382**, 80-83.
- Trupp, M., Arenas, E., Fainzilber, M., Nilsson, A.-S., Sieber, B.-A., Grigoriou, M., Kilkenny, C., Salazar-Gruoso, E., Pachnis, V., Arumäe, U. et al. (1996). Functional receptor for GDNF encoded by the c-ret proto-oncogene. *Nature* **381**, 785-789.
- Uesaka, T., Jain, S., Yonemura, S., Uchiyama, Y., Milbrandt, J. and Enomoto, H. (2007). Conditional ablation of GFR α 1 in postmigratory enteric neurons triggers unconventional neuronal death in the colon and causes a Hirschsprung's disease phenotype. *Development* **134**, 2171-2181.
- Vergaño-Vera, E., Yusta-Boyo, M. J., de Castro, F., Bernad, A., de Pablo, F. and Vicario-Abejón, C. (2006). Generation of GABAergic and dopaminergic interneurons from endogenous embryonic olfactory bulb precursor cells. *Development* **133**, 4367-4379.
- Waclaw, R. R., Allen, Z. J., Bell, S. M., Erdélyi, F., Szabó, G., Potter, S. S. and Campbell, K. (2006). The zinc finger transcription factor Sp8 regulates the generation and diversity of olfactory bulb interneurons. *Neuron* **49**, 503-516.
- Wichterle, H., Turnbull, D. H., Nery, S., Fishell, G. and Alvarez-Buylla, A. (2001). In utero fate mapping reveals distinct migratory pathways and fates of neurons born in the mammalian basal forebrain. *Development* **128**, 3759-3771.
- Young, K. M., Fogarty, M., Kessar, N. and Richardson, W. D. (2007). Subventricular zone stem cells are heterogeneous with respect to their embryonic origins and neurogenic fates in the adult olfactory bulb. *J. Neurosci.* **27**, 8286-8296.



Supplementary Figure 1. Loss of GFR α 1 expression in septum of R1CG mice after Cre-mediated recombination driven by *Gad67*^{Cre}

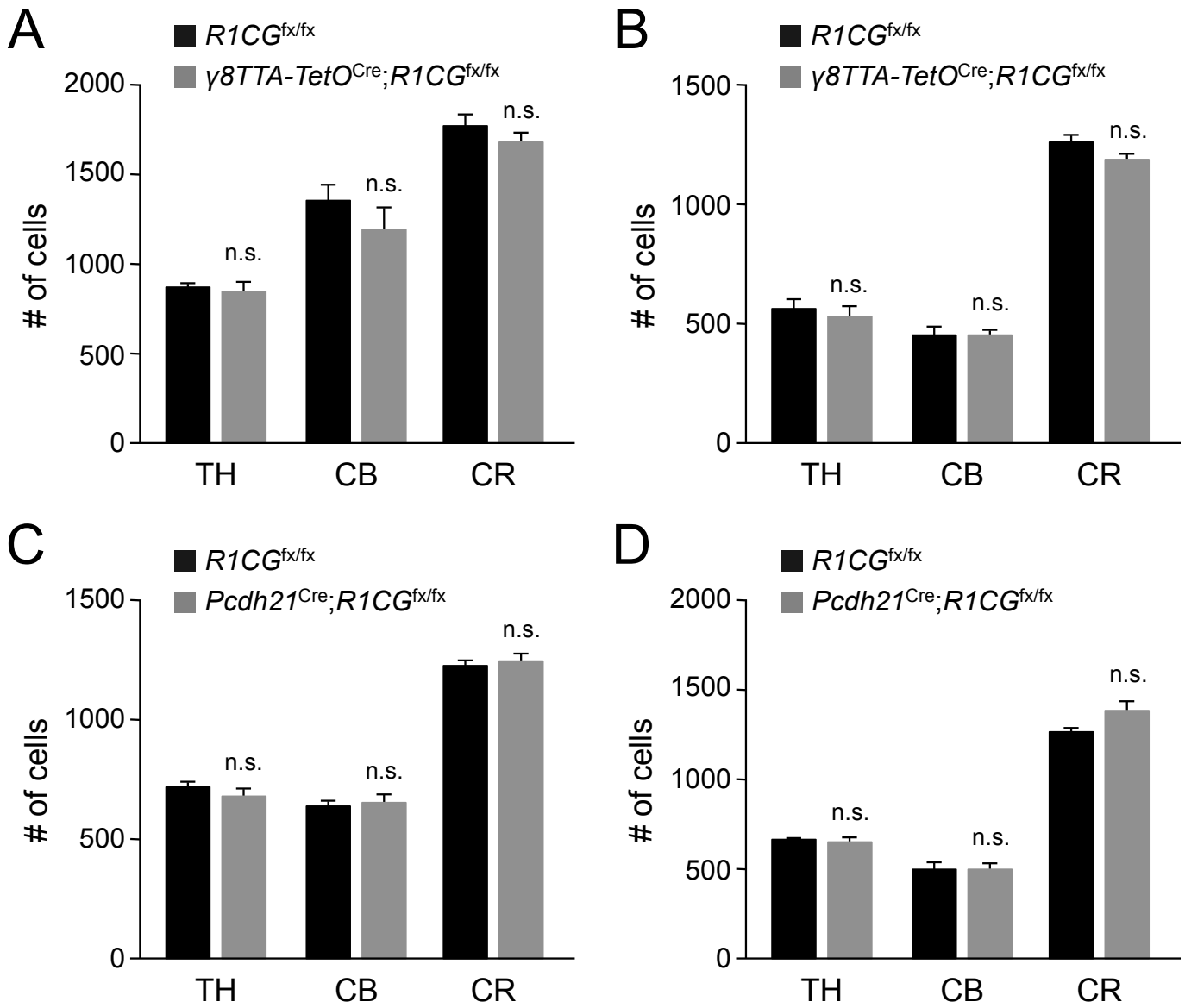
Images derived from the septal area of 7-week old mice. GFP is expressed from the *Gfra1* locus after recombination. Scale bars, 300 μ m (leftpanels), 75 μ m (insets).



Supplementary Figure 2. Loss of mature OSNs in olfactory epithelium of *γ8TTA-TetO^{Cre};R1CG^{fx/fx}* conditional mutant mice

(A) Representative images of olfactory epithelium of P56 *γ8TTA-TetO^{Cre};R1CG^{fx/fx}* conditional mutant and *R1CG^{fx/fx}* control mice immunostained for OMP (green, marking mature OSNs) and GAP43 (red, marking immature OSNs). OSN axon bundles can be seen in the lamina propia. Scale bar, 50 μ m.

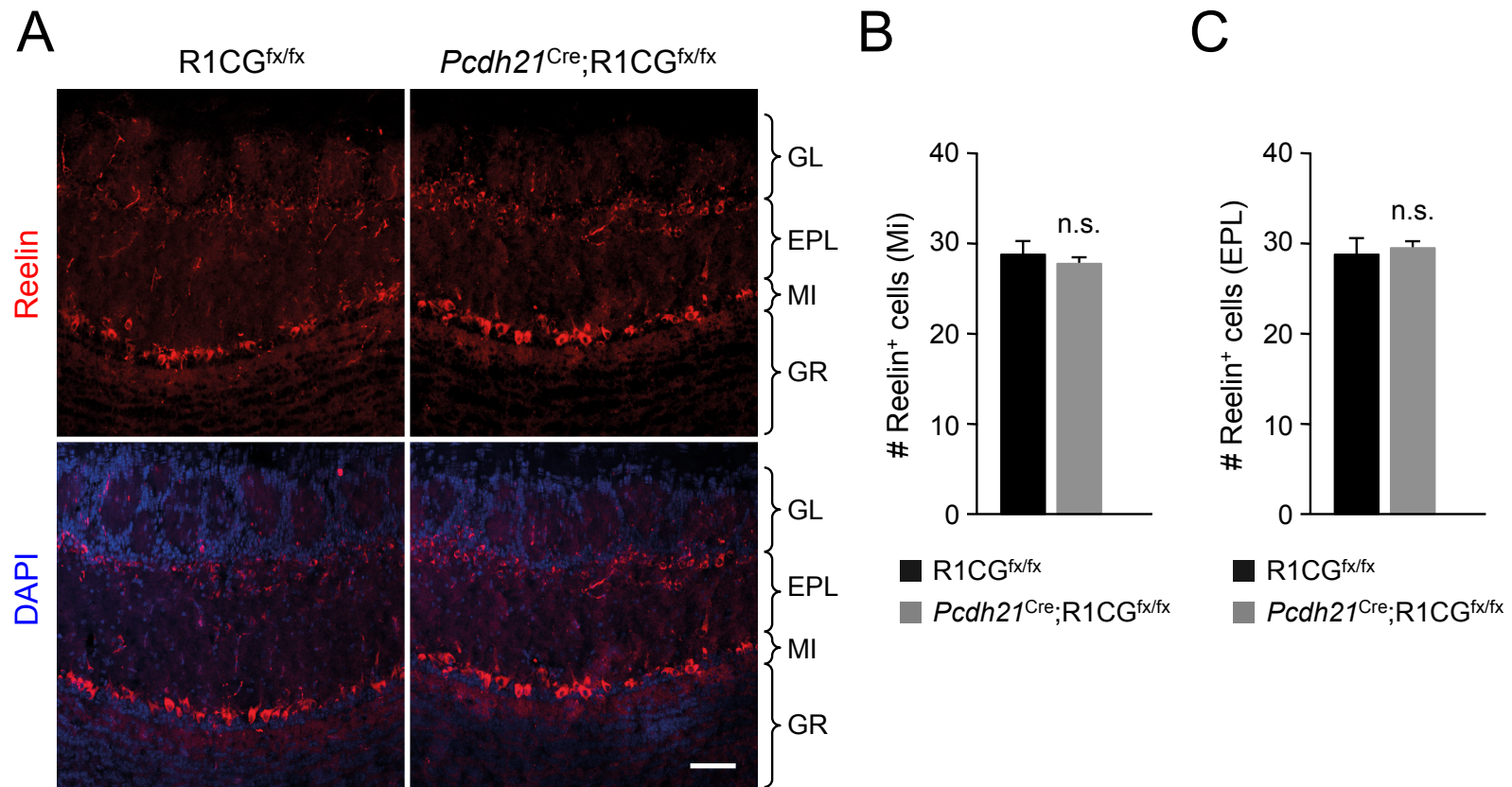
(B) Quantification of mature OSNs (mOSNs) in the olfactory epithelium of P56 *γ8TTA-TetO^{Cre};R1CG^{fx/fx}* conditional mutant and *R1CG^{fx/fx}* control mice. N = 6 mice per group. ***, $p < 0.0005$.



Supplementary Figure 3. No loss of OB GABAergic interneurons in conditional mutants lacking GFR α 1 in OSNs or projection neurons

(A, C) Quantification of the number of cells expressing TH, Calbindin (CB) and Calretinin (CR) in the OB of newborn $\gamma 8TTA-TetO^{Cre};R1CG^{fx/fx}$ (A) and $Pcdh21^{Cre};R1CG^{fx/fx}$ (C) conditional mutants and $R1CG^{fx/fx}$ control mice. The values represent total number of cells in fields encompassing the entire OB. N = 3 mice per group; n.s., not significantly different.

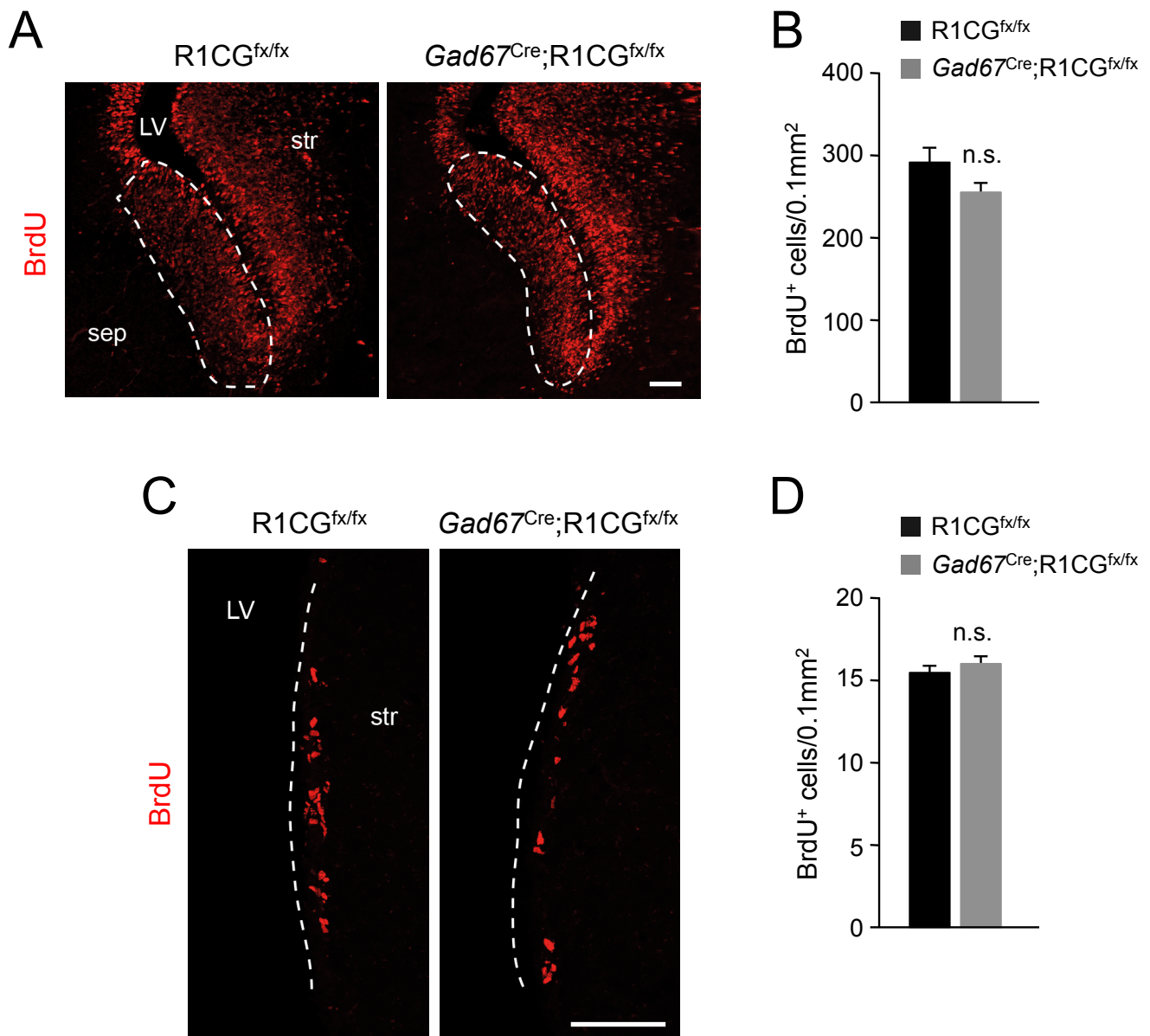
(B, D) Quantification of the number of cells expressing TH, Calbindin (CB) and Calretinin (CR) in the OB of P56 $\gamma 8TTA-TetO^{Cre};R1CG^{fx/fx}$ (B) and $Pcdh21^{Cre};R1CG^{fx/fx}$ (D) conditional mutants and $R1CG^{fx/fx}$ control mice. The values represent number of cells counted in the glomerular layer of the medial surface of the OB (see Materials and Methods for details). N = 3 mice per group; n.s., not significantly different.



Supplementary Figure 4. No loss of projection neurons in the OB of *Pcdh21*^{Cre};R1CG^{fx/fx} conditional mutant mice

(A) Representative images of the OB of P56 *Pcdh21*^{Cre};R1CG^{fx/fx} conditional mutant and R1CG^{fx/fx} control mice immunostained for Reelin (red), marking mitral cells in Mi layer and tufted cells in the EPL. GL, glomerular layer; EPL, external plexiform layer; MI, mitral cell layer; GR, granule cell layer; Scale bar, 100 μ m.

(B, C) Quantification of Reelin⁺ cells in the mitral cell layer (B), i.e. mitral cells, and in the external plexiform layer (C), i.e. external tufted cells, of the OB of P56 *Pcdh21*^{Cre};R1CG^{fx/fx} conditional mutant and R1CG^{fx/fx} control mice. N = 5 mice per group. n.s., not significantly different.



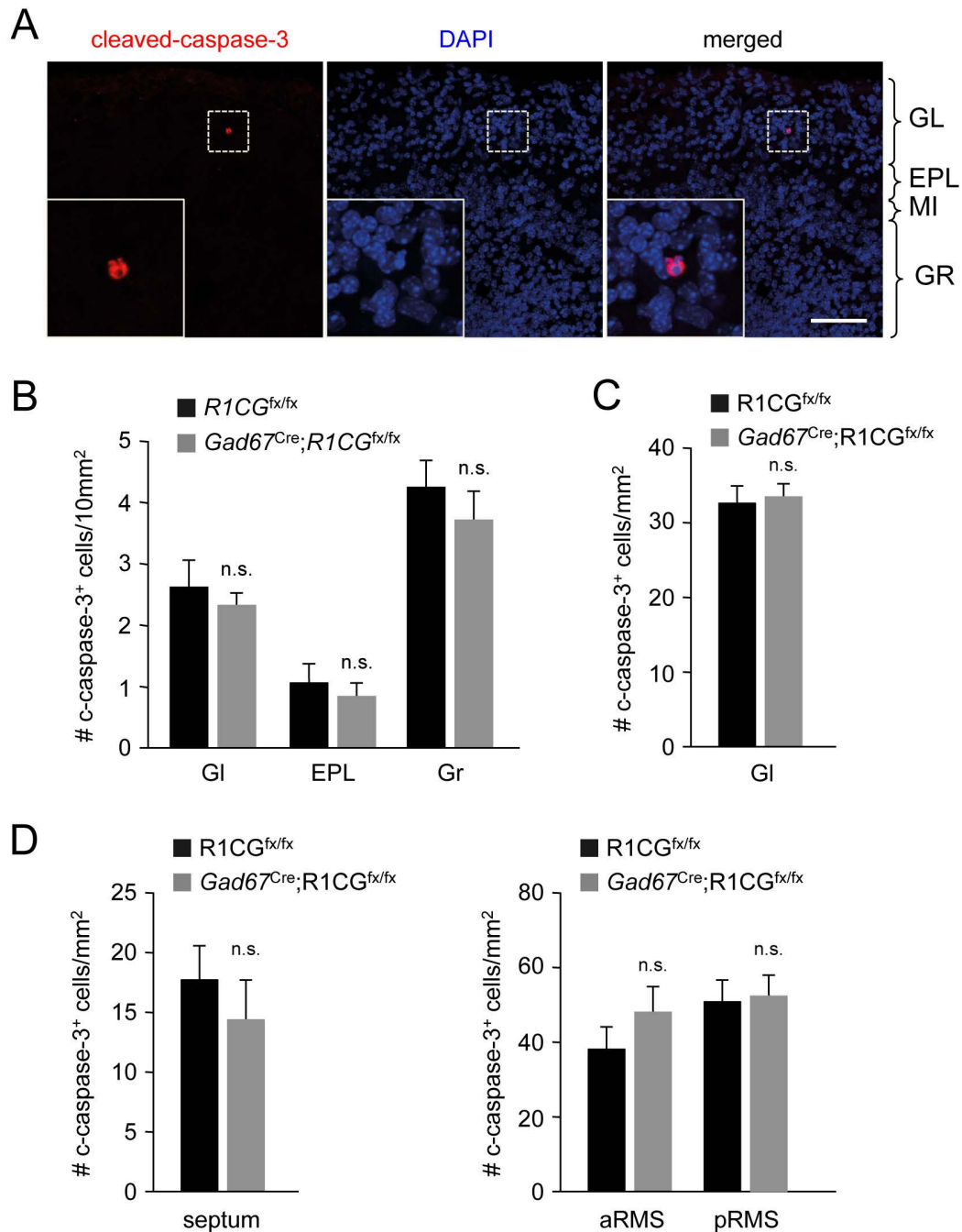
Supplementary Figure 5. Normal proliferation of precursors in embryonic septum and adult SVZ in conditional mutant mice lacking GFR α 1 in GABAergic cells

(A) Representative images of BrdU immunostaining from the septal ventricular zone (VZ, dashed line) of E16.5 *Gad67*^{Cre};R1CG^{fx/fx} conditional mutant and R1CG^{fx/fx} control embryos 30 min after a BrdU injection. LV, lateral ventricle; sep, septum; str, striatum. Scale bar, 100 μ m.

(B) Quantification of BrdU positive cells in the septal VZ of septum of E16.5 *Gad67*^{Cre};R1CG^{fx/fx} conditional mutant and R1CG^{fx/fx} control embryos 30 min after a BrdU injection. N = 5 embryos per group. n.s., not significantly different.

(C) Representative images of BrdU immunostaining from the subventricular zone (SVZ) of the lateral ventricle wall of P56 *Gad67*^{Cre};R1CG^{fx/fx} conditional mutant and R1CG^{fx/fx} control mice 1 hour after a BrdU injection. LV, lateral ventricle; str, striatum. Scale bar, 100 μ m.

(D) Quantification of BrdU positive cells in the SVZ of the lateral ventricle wall of P56 *Gad67*^{Cre};R1CG^{fx/fx} conditional mutant and R1CG^{fx/fx} control mice 1 hour after a BrdU injection. N = 5 embryos per group. n.s., not significantly different.



Supplementary Figure 6. Unaltered cell death in conditional mutant mice lacking GFR α 1 in GABAergic cells

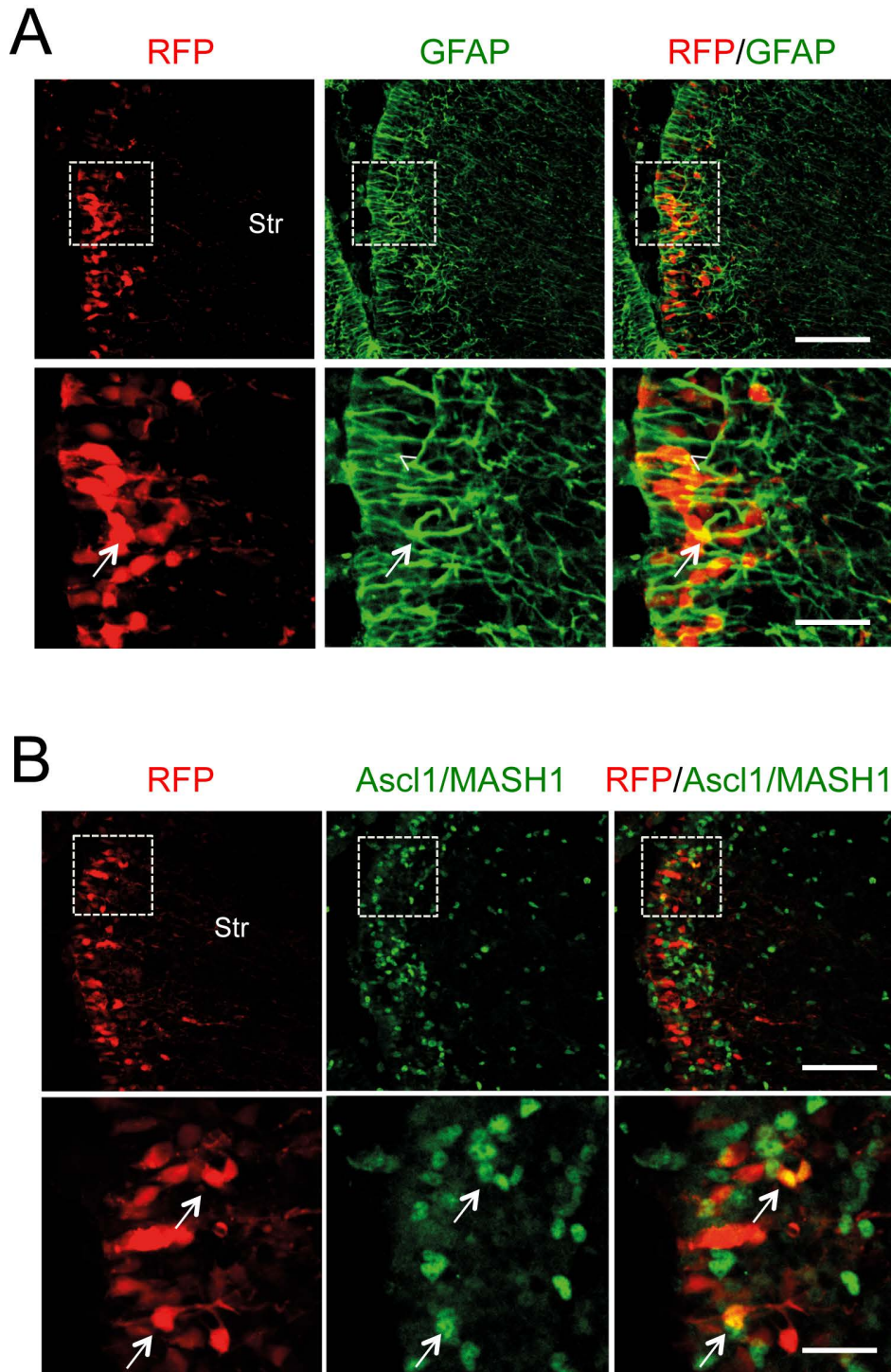
(A) Representative images of immunostaining for cleaved caspase-3 (red) and DAPI (blue) in the OB of newborn wild type mice. Insets show high magnification of boxed areas. Scale bar, 50 μ m.

(B) Quantification of cleaved-caspase-3 in the OB of E16.5 $Gad67^{Cre};R1CG^{fx/fx}$ conditional mutant and $R1CG^{fx/fx}$ control embryos. GL, glomerular layer; EPL, external plexiform layer; GR, granule cell layer; M, mitral cell layer. N = 5 embryos per group. n.s., not significantly different.

(C) Quantification of cleaved-caspase-3 in the medial surface of the glomerular layer of P56 $Gad67^{Cre};R1CG^{fx/fx}$ conditional mutant and $R1CG^{fx/fx}$ control mice. GI, glomerular layer. N = 5 mice per group. n.s., not significantly different.

(D) Quantification of cleaved-caspase-3 in the septum of E16.5 $Gad67^{Cre};R1CG^{fx/fx}$ conditional mutant and $R1CG^{fx/fx}$ control embryos. N = 5 embryos per group. n.s., not significantly different.

(E) Quantification of cleaved-caspase-3 in the anterior and posterior RMS of P56 $Gad67^{Cre};R1CG^{fx/fx}$ conditional mutant and $R1CG^{fx/fx}$ control mice. N = 5 mice per group. n.s., not significantly different.



Supplementary Figure 7. Targeting of precursor cells in the ventricular wall of neonate mice by *in vivo* electroporation
 (A, B) Representative images of expression of RFP (red, marking electroporated cells) and GFAP (A) or Ascl1/MASH1 (B) (green, marking type C transit amplifying cells) in the SVZ two days after ventricular electroporation of a RFP-expressing plasmid in new born wild type mice. Bottom row panels show high magnification of boxed areas. Arrows indicate double positive cells. Scale bar, 50 μ m (upper panels), 25 μ m (lower panels).